EUROPEAN PHYSICAL SOCIETY EPS HEP2025 MARSEILLE

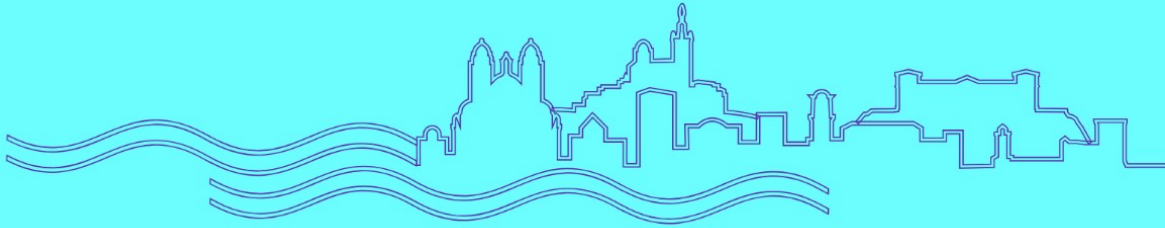

Charged-particle production in pp collisions at $\sqrt{s}$ = 13.6 TeV and Pb–Pb collisions at $\sqrt{s_{NN}}$ = 5.36 TeV with ALICE

Abhi Modak on behalf of ALICE Collaboration

INFN – Sezione di Trieste, Italy

Email: abhi.modak@cern.ch

INFN Istituto Nazionale di Fisica Nucleare

ALICE

Focus of the talk:

→ Charged-particle multiplicity density ($dN_{ch}/d\eta$)

→ Mid and forward rapidity

Importance of multiplicity

☆ Fundamental observable to understand the particle production mechanisms

Soft QCD processes

- Low p_T, non-perturbative
- Phenomenology and modeling

Hard QCD processes

- High p_T, perturbative
- Described by pQCD calculation

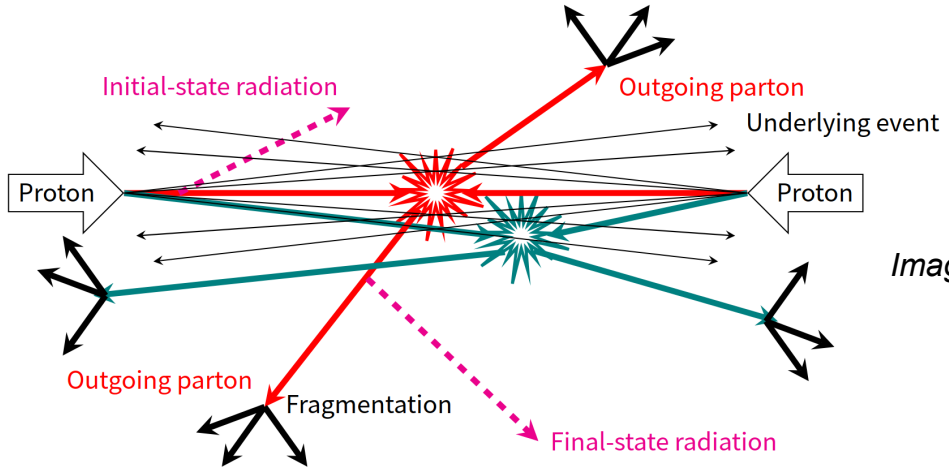

Image from A. Alkin, QM22

Importance of multiplicity

☆ Fundamental observable to understand the particle production mechanisms

Soft QCD processes
- ❑ Low p_T, non-perturbative
- ❑ Phenomenology and modeling

Hard QCD processes
- ❑ High p_T, perturbative
- ❑ Described by pQCD calculation

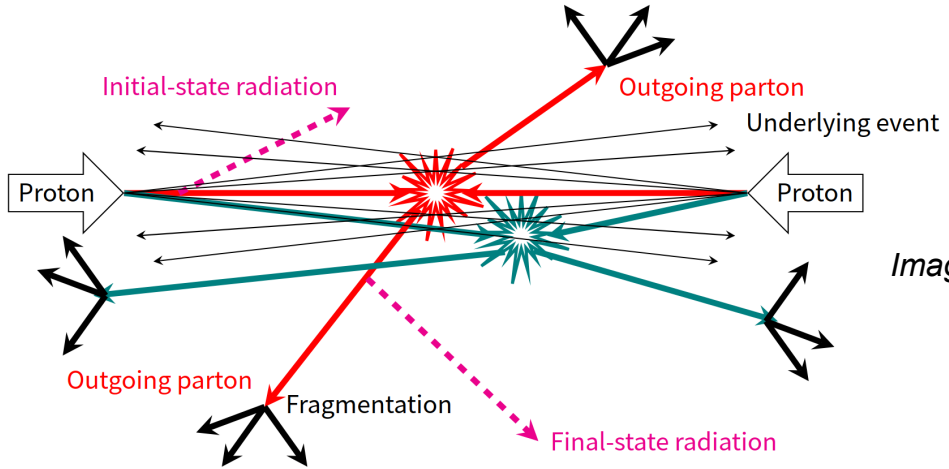

Image from A. Alkin, QM22

☆ Carrying important information of
- →Energy density in the initial-state
- →Centrality of the collision

$$\epsilon = \frac{\mathrm{d}E_T/\mathrm{d}y}{\tau\,\pi\,R^2} \sim \frac{3}{2}\langle m_T \rangle \frac{\mathrm{d}N_{ch}/\mathrm{d}\eta}{\tau\,\pi\,R^2}$$

J. D. Bjorken, PRD 27 (1983) 140–151

Importance of multiplicity

☆ Fundamental observable to understand the particle production mechanisms

Soft QCD processes
- ❑ Low p_T, non-perturbative
- ❑ Phenomenology and modeling

Hard QCD processes
- ❑ High p_T, perturbative
- ❑ Described by pQCD calculation

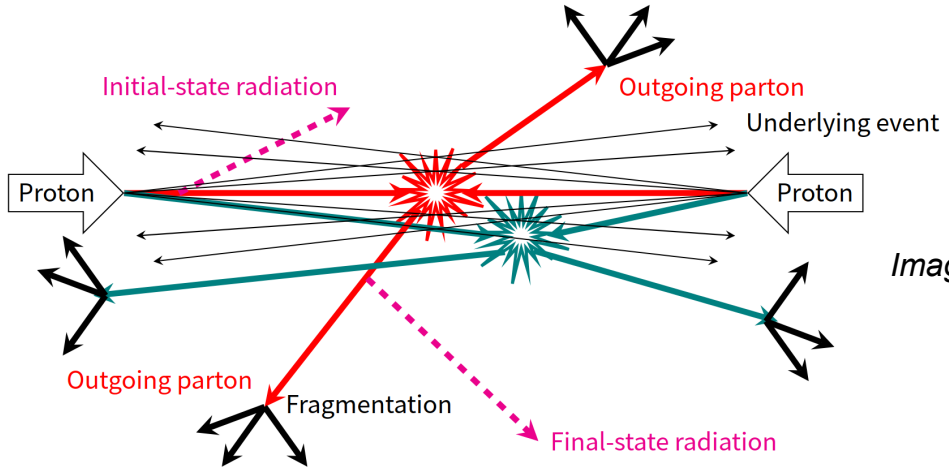

Image from A. Alkin, QM22

☆ Carrying important information of
- →Energy density in the initial-state
- →Centrality of the collision

$$\epsilon = \frac{\mathrm{d}E_T/\mathrm{d}y}{\tau\,\pi\,R^2} \sim \frac{3}{2}\langle m_T \rangle \frac{\mathrm{d}N_{ch}/\mathrm{d}\eta}{\tau\,\pi\,R^2}$$

J. D. Bjorken, PRD 27 (1983) 140–151

☆ Good input for constraining theoretical models

A Large Ion Collider Experiment

- Continuous readout of all detectors
- New online-offline (O^2) framework

ALICE in Run 3

ALICE, JINST 19 (2024) P05062

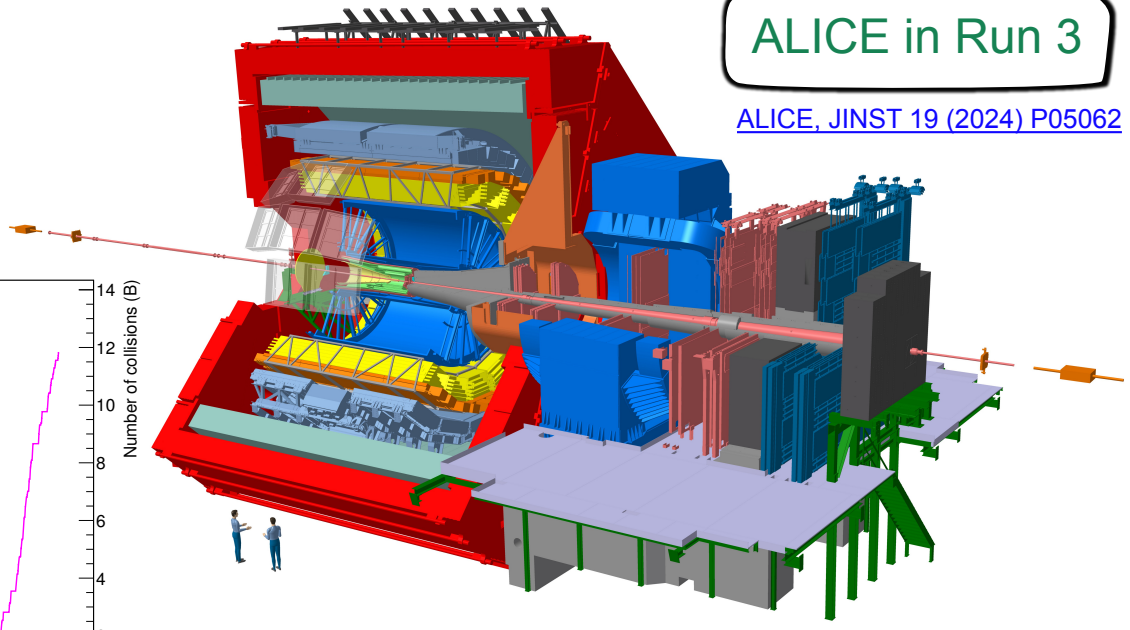

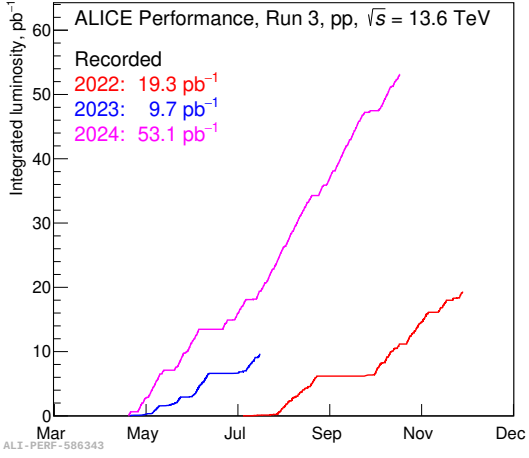

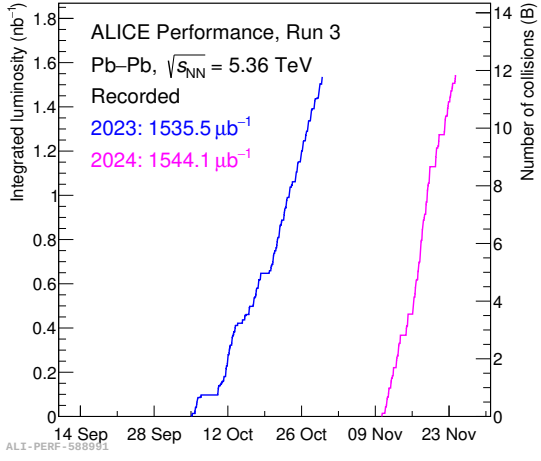

- 82 pb^{-1} recorded for pp (~2.5k times larger than Run 1+2)
- 3.08 nb^{-1} recorded for Pb–Pb (~75 times larger than Run 1+2)

This analysis uses sub-sample of

- pp 2022 data
- Pb–Pb 2023 data

A Large Ion Collider Experiment

Measure N_{ch} at midrapidity

Inner Tracking System (ITS2)

- 7 layers of silicon pixel sensors
- Tracking and vertexing
- $|\eta| < 1.3$

Time Projection Chamber (TPC)

- GEM-based readout pads
- Tracking and PID
- $|\eta| < 0.9$

ALICE in Run 3

ALICE, JINST 19 (2024) P05062

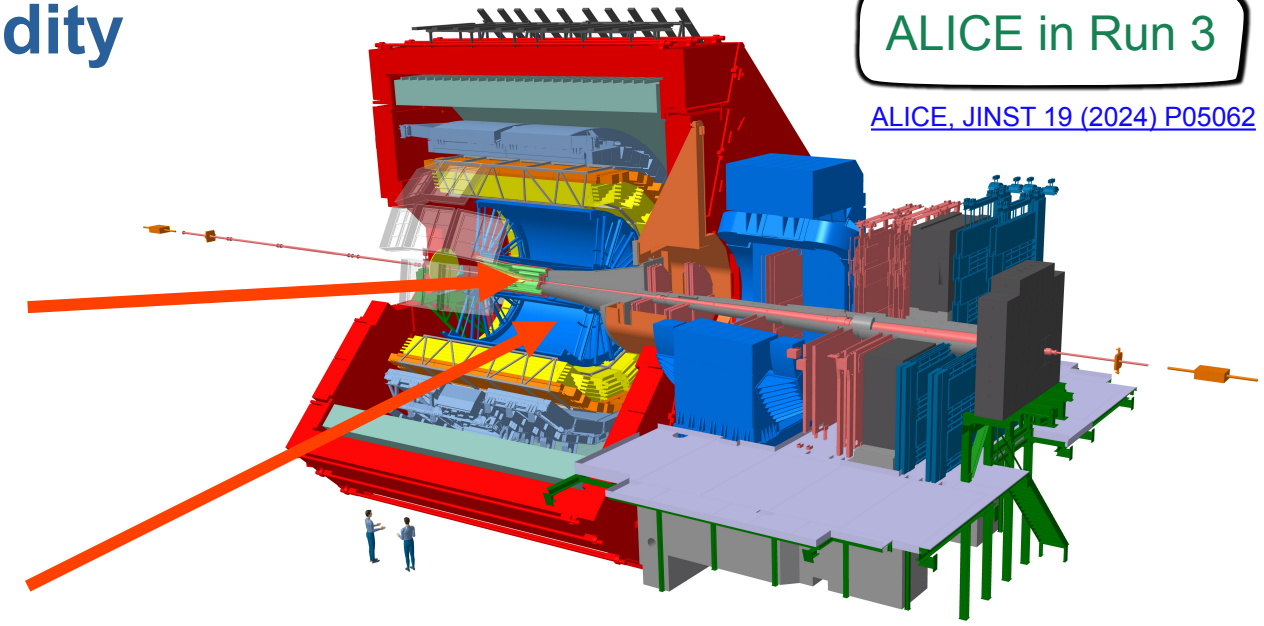

Track selection

- → Global tracks: Best quality tracks that are matched between ITS and TPC
- → ITS-only tracks

Measure N_{ch} at forward rapidity

ALICE in Run 3

ALICE, JINST 19 (2024) P05062

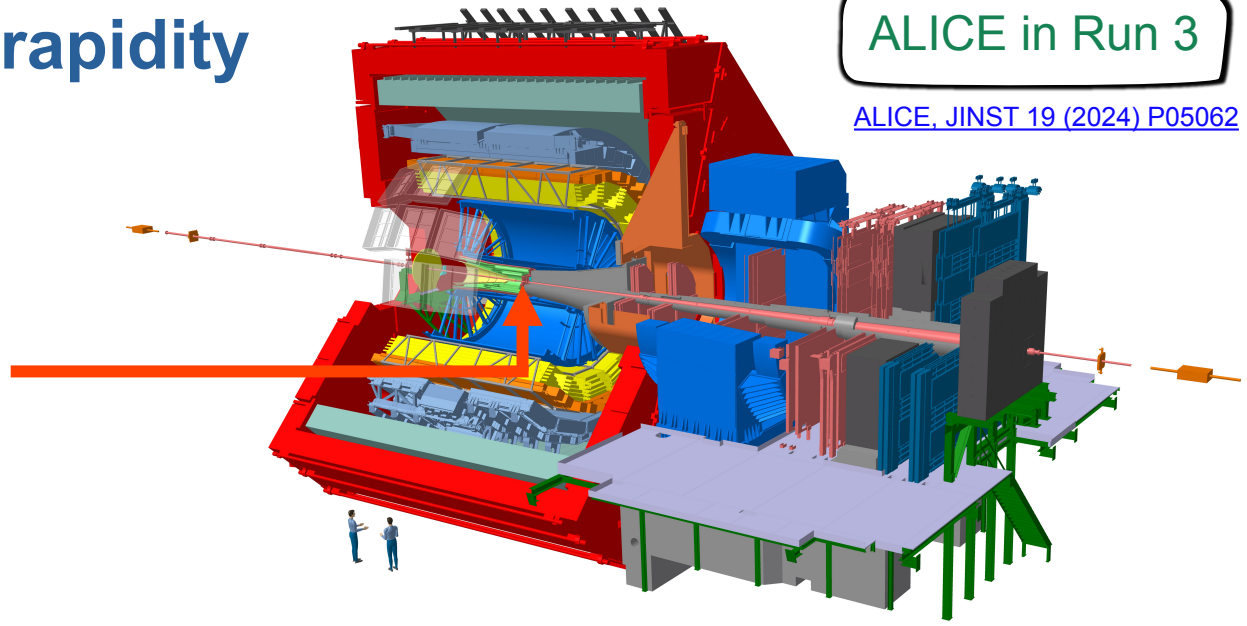

Muon Forward Tracker (MFT)

- 5 detection disks, 2 detection planes each
- Vertexing for muons
- $-3.6 < \eta < -2.4$

Track selection

→ Hits on at least 5 planes of MFT

Centrality determination

Fast Interaction Trigger (FIT)

- Collision time, event selection and centrality estimation
- Three sub-detectors – FT0, FV0 and FDD
- FT0C ($-3.3 < \eta < -2.1$)

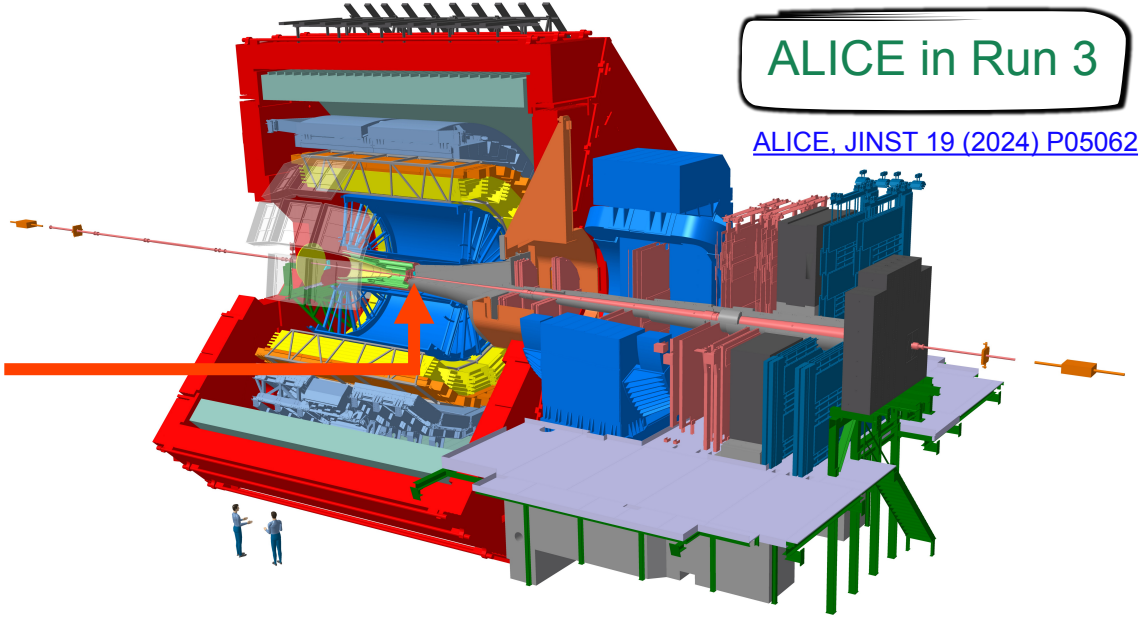

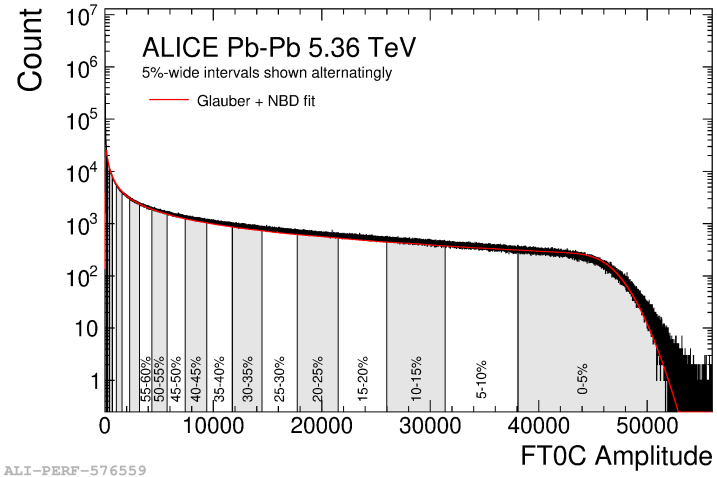

Centrality determination

Fast Interaction Trigger (FIT)

- Collision time, event selection and centrality estimation
- Three sub-detectors – FT0, FV0 and FDD
- FT0C (-3.3 < η < -2.1)

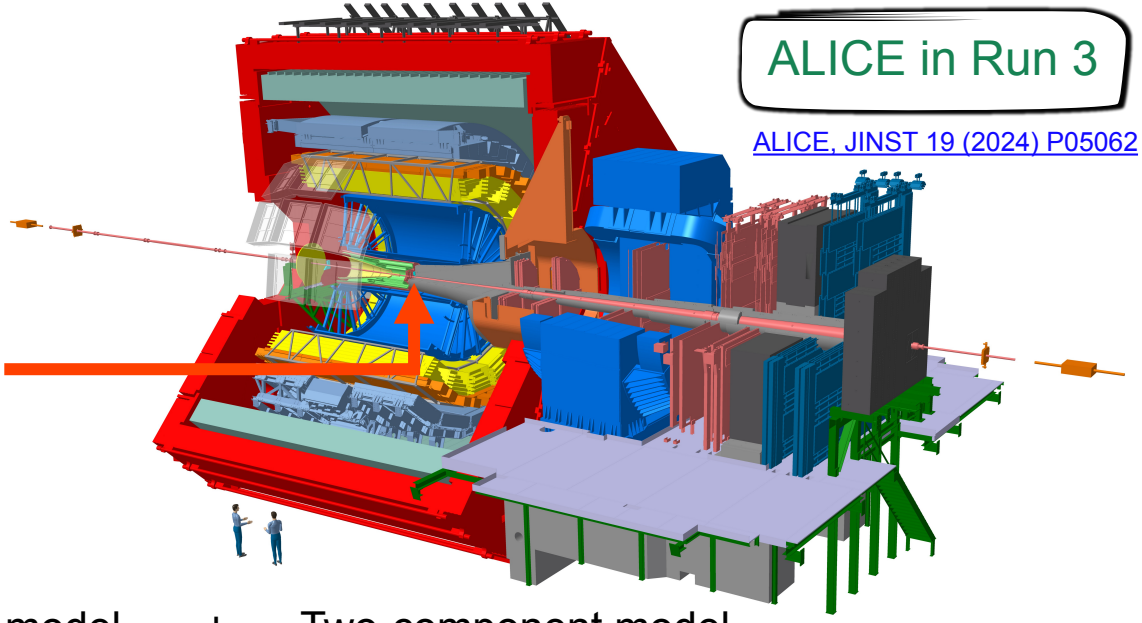

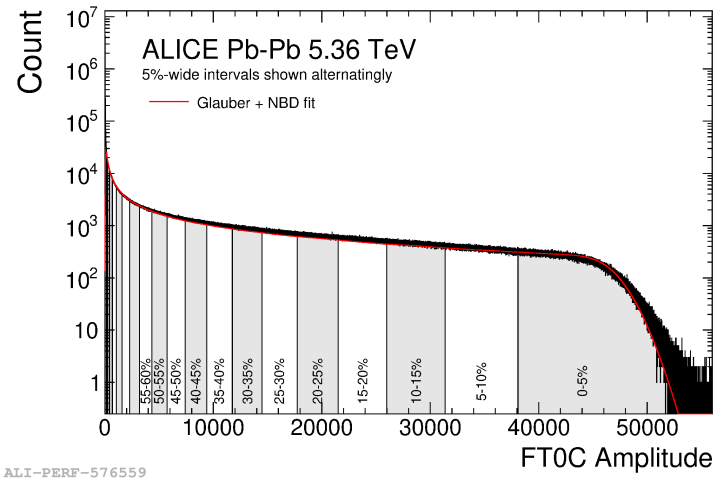

Glauber model + Two-component model

Centrality determination

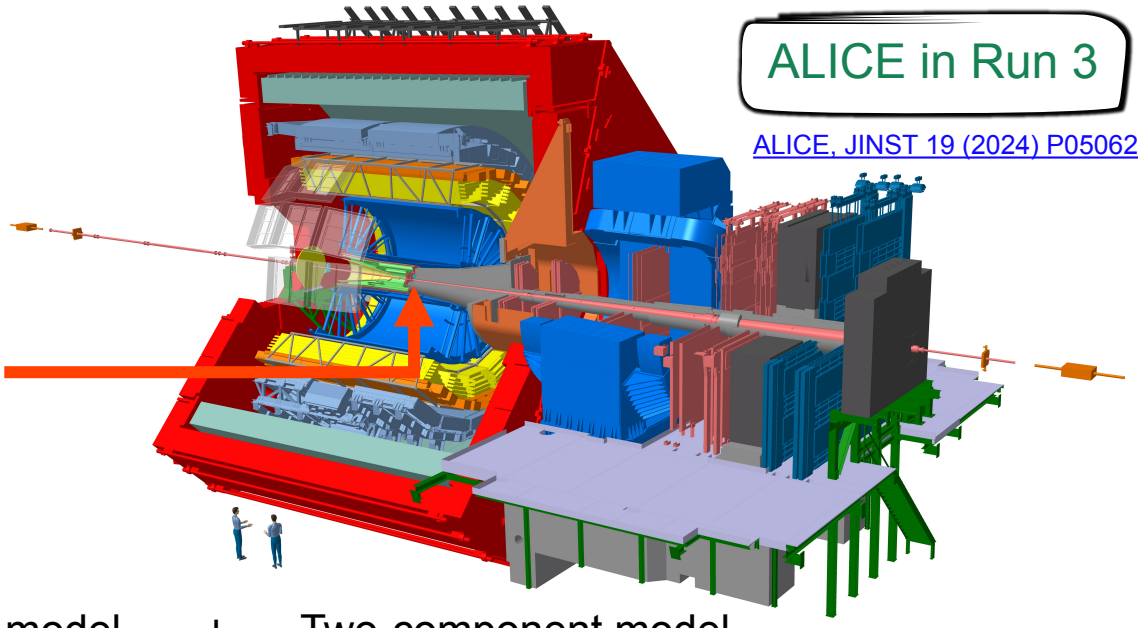

Fast Interaction Trigger (FIT)

- Collision time, event selection and centrality estimation
- Three sub-detectors – FT0, FV0 and FDD
- FT0C (-3.3 < η < -2.1)

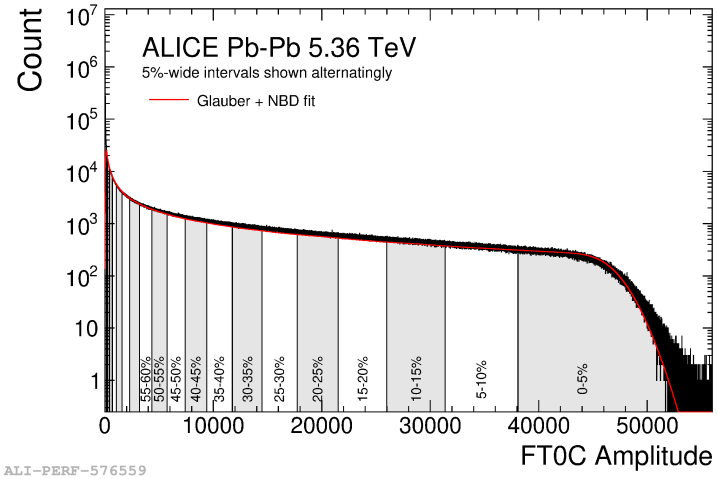

ALI-PERF-576559

Glauber model + Two-component model

$$\rho(r) = \rho_0 \frac{1 + w(r/R)^2}{1 + \exp\left(\frac{r-R}{a}\right)}$$

Nuclear radius (***R***) = 6.62 ± 0.06 fm
Skin thickness (***a***) = 0.546 ± 0.010 fm
σ_{INEL} = 68.2 ± 0.6 mb

Centrality determination

Fast Interaction Trigger (FIT)

- Collision time, event selection and centrality estimation
- Three sub-detectors – FT0, FV0 and FDD
- FT0C (-3.3 < η < -2.1)

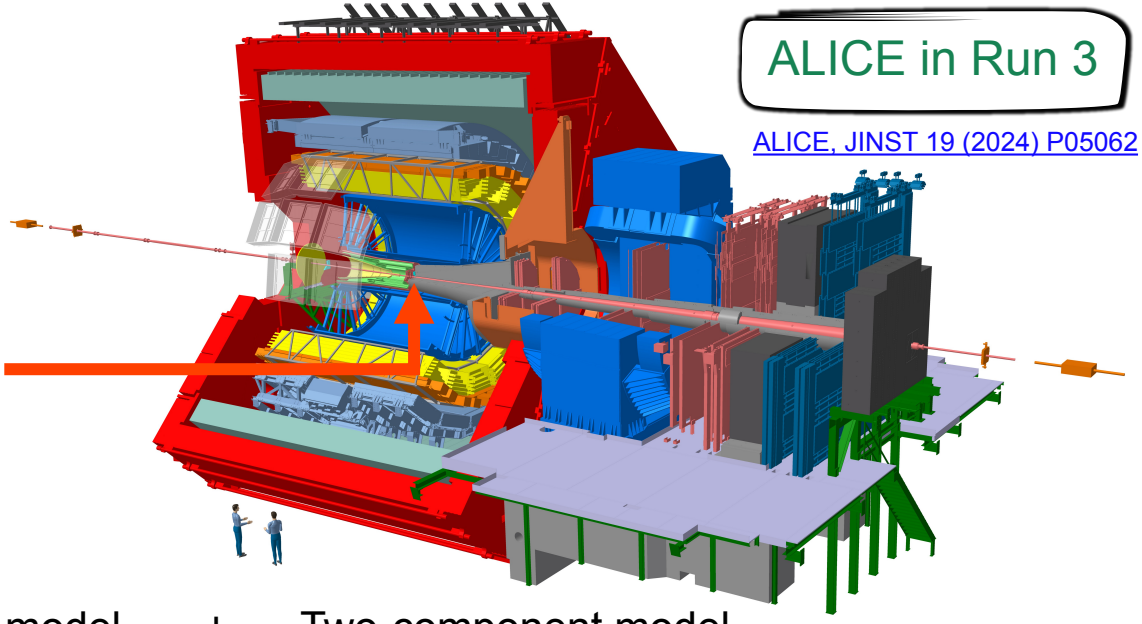

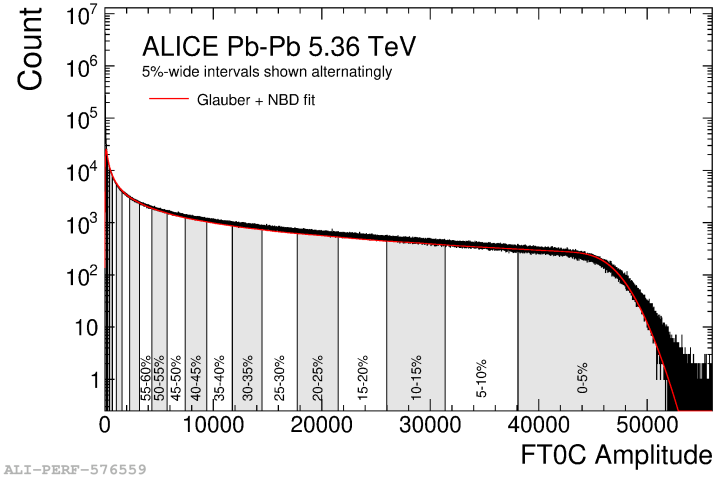

Glauber model + Two-component model

$$\rho(r) = \rho_0 \frac{1 + w(r/R)^2}{1 + \exp\left(\frac{r-R}{a}\right)}$$

$$N_{\text{sources}} = f \times N_{\text{part}} + (1 - f) \times N_{\text{coll}}$$

Particle produced by each source is parameterised by negative binomial distribution (NBD)

Nuclear radius (***R***) = 6.62 ± 0.06 fm
Skin thickness (***a***) = 0.546 ± 0.010 fm
σ_{INEL} = 68.2 ± 0.6 mb

Centrality determination

Fast Interaction Trigger (FIT)

- Collision time, event selection and centrality estimation
- Three sub-detectors – FT0, FV0 and FDD
- FT0C (-3.3 < η < -2.1)

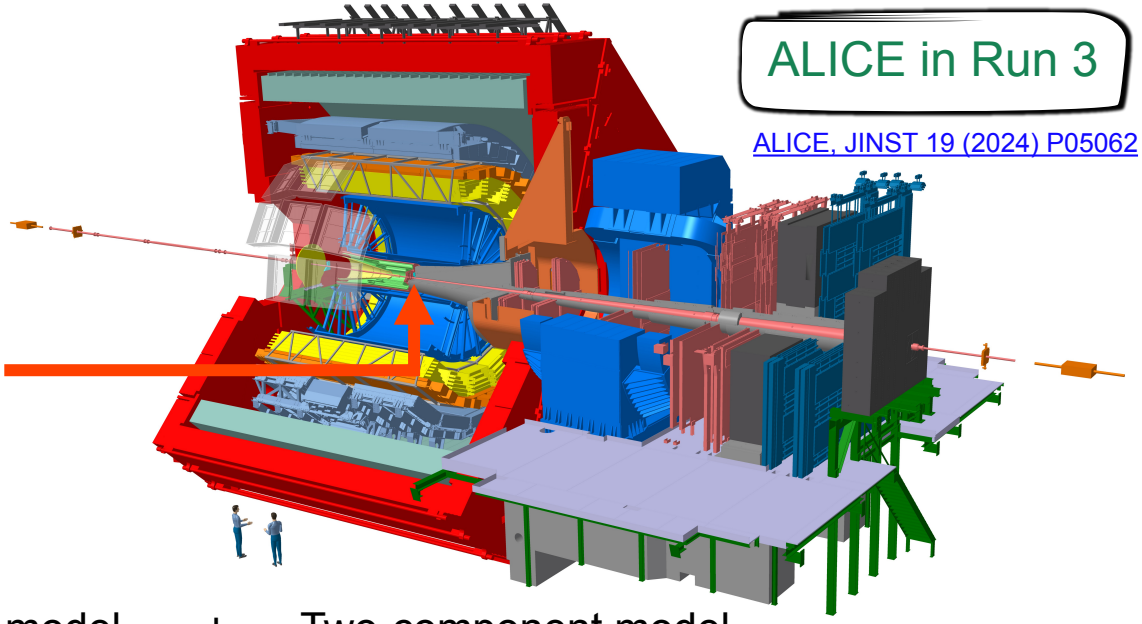

ALICE in Run 3

ALICE, JINST 19 (2024) P05062

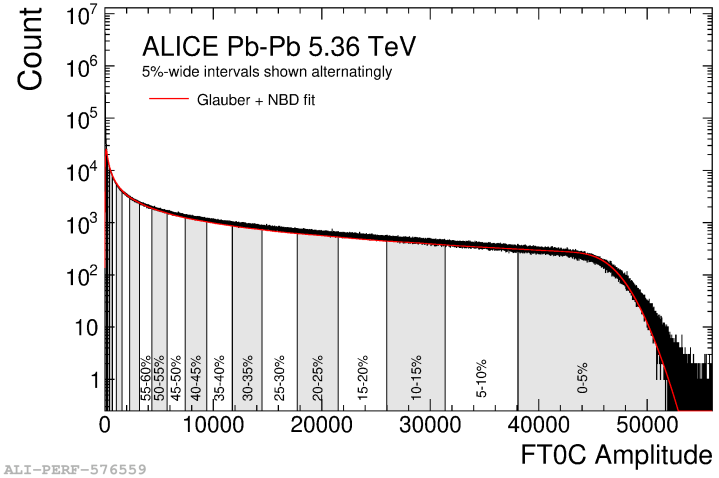

ALI-PERF-576559

Glauber model + Two-component model

$$\rho(r) = \rho_0 \frac{1 + w(r/R)^2}{1 + \exp\left(\frac{r-R}{a}\right)}$$

$$N_{\text{sources}} = f \times N_{\text{part}} + (1 - f) \times N_{\text{coll}}$$

Particle produced by each source is parameterised by negative binomial distribution (NBD)

Nuclear radius (***R***) = 6.62 ± 0.06 fm
Skin thickness (***a***) = 0.546 ± 0.010 fm
σ_{INEL} = 68.2 ± 0.6 mb

The NBD-Glauber fit provides a good description of data

Results from pp collisions

$dN_{ch}/d\eta$ in pp collisions

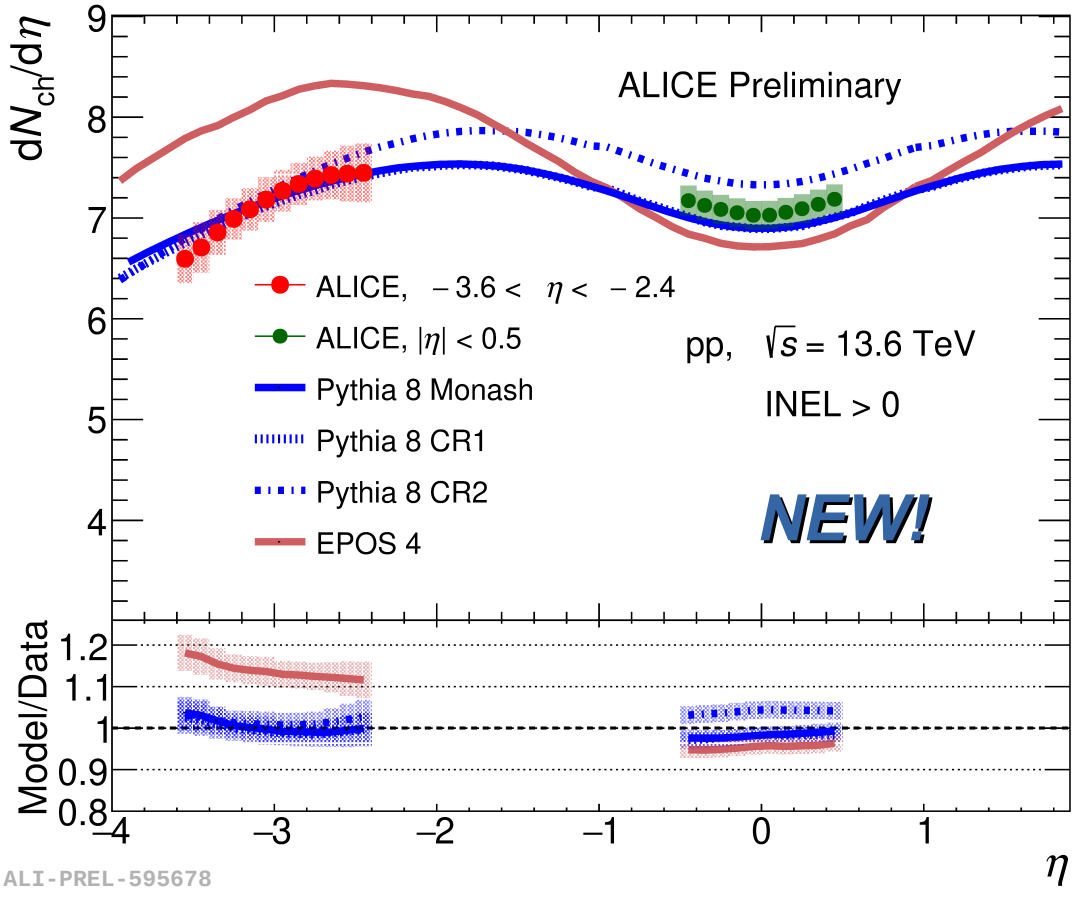

$dN_{ch}/d\eta$ in pp collisions

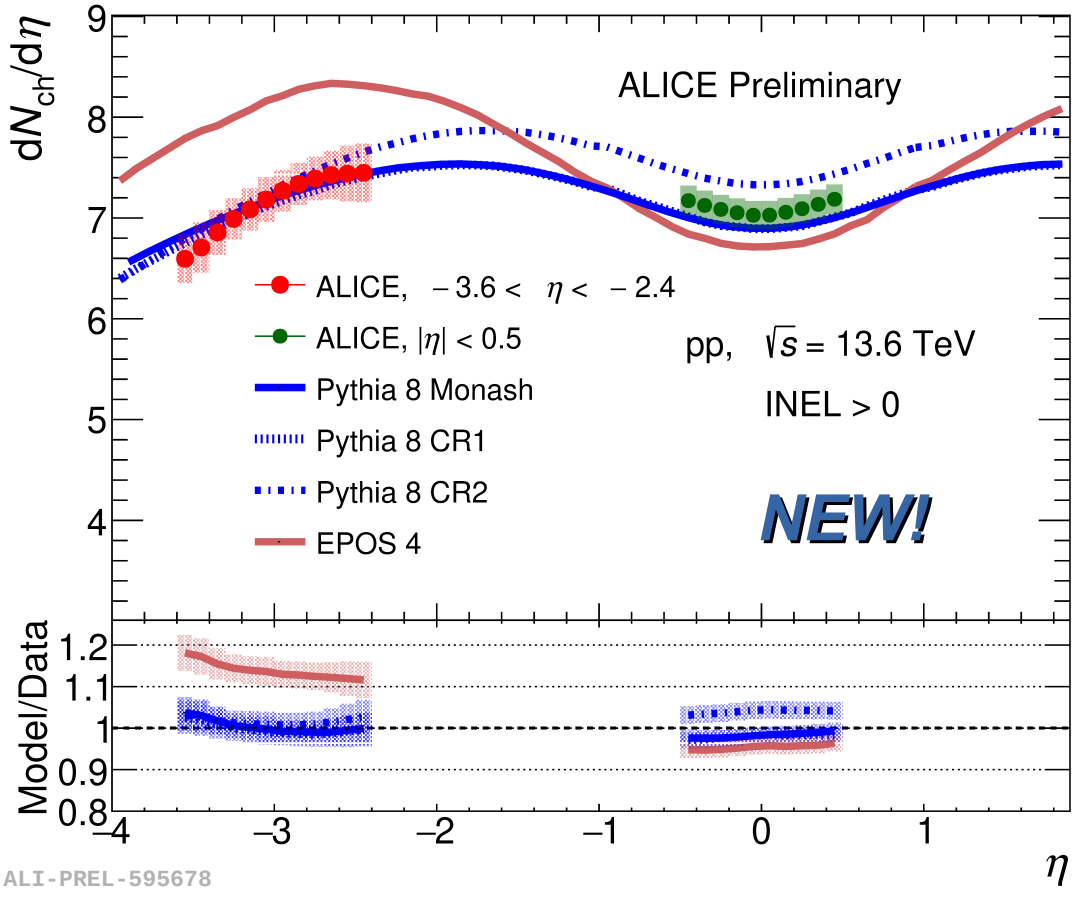

INEL > 0:

→ Inelastic events having at least one charged particle in $|\eta| < 1$

$dN_{ch}/d\eta$ in pp collisions

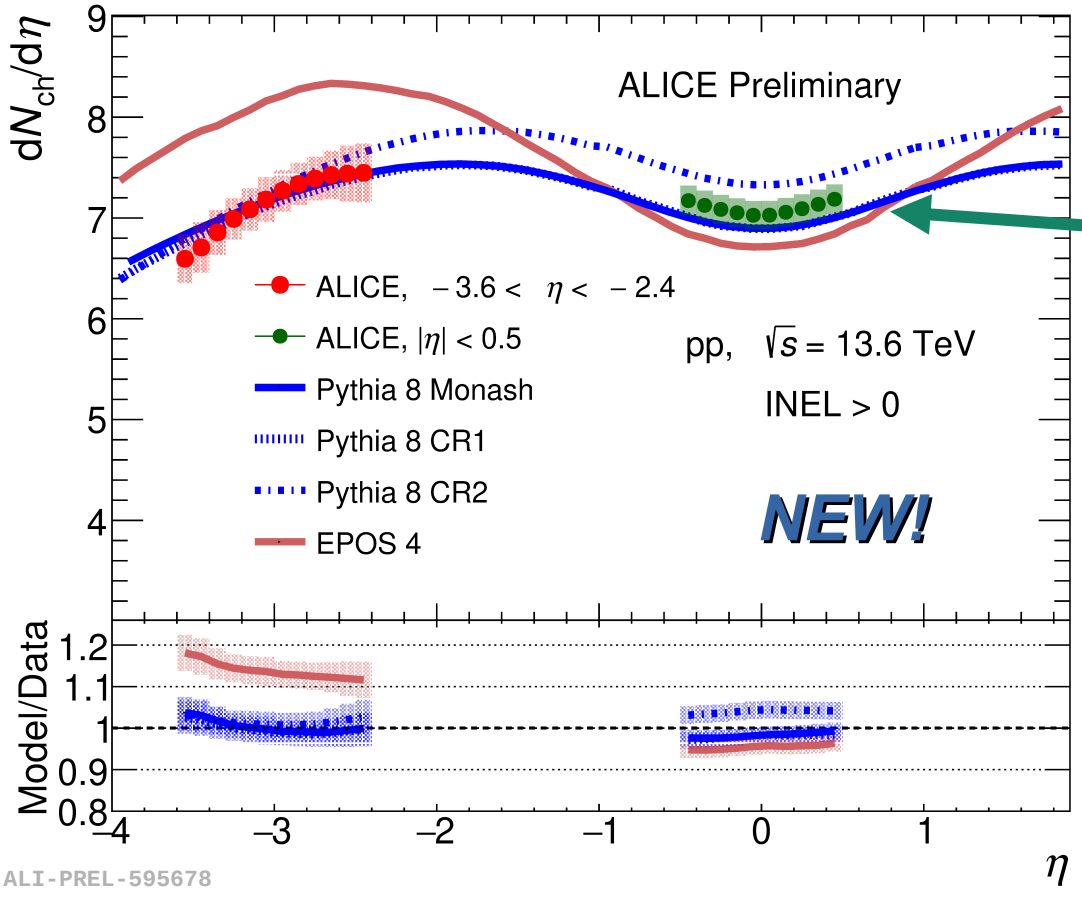

INEL > 0:

→ Inelastic events having at least one charged particle in $|\eta| < 1$

Midrapidity ($|\eta| < 0.5$) results

$dN_{ch}/d\eta$ in pp collisions

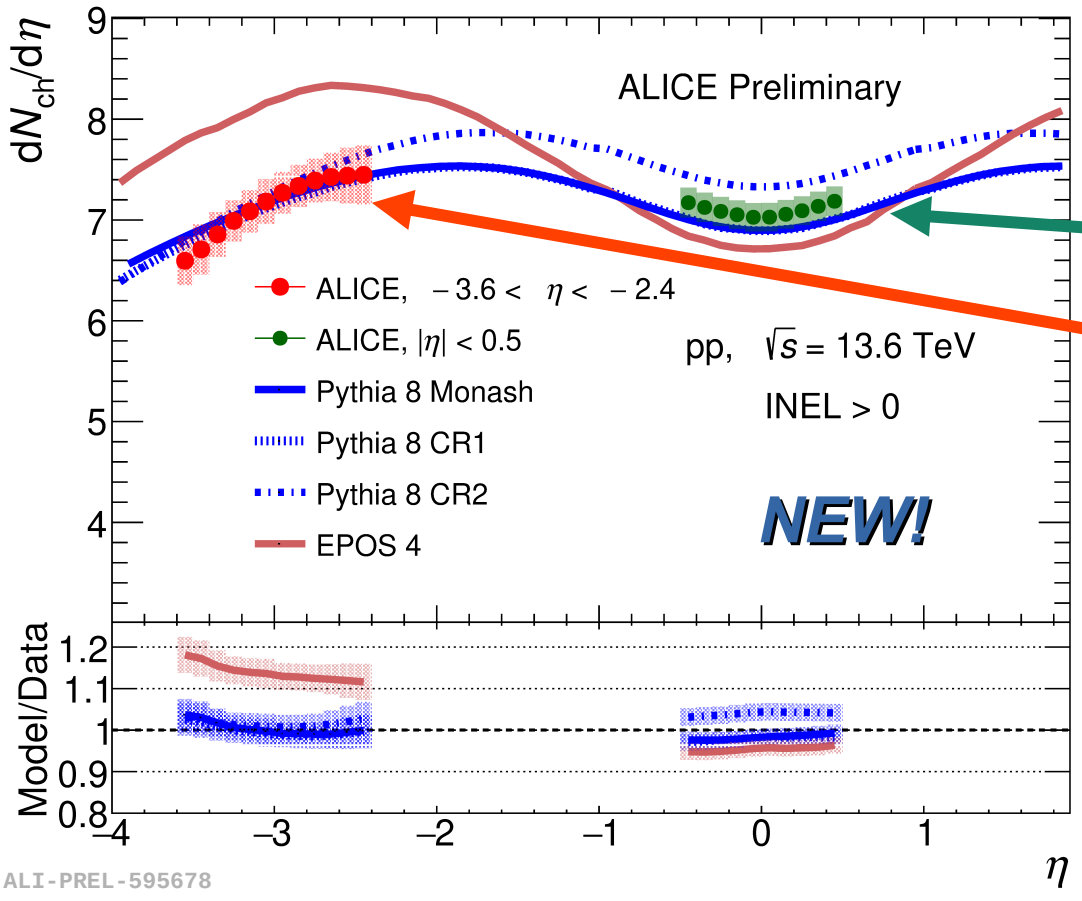

INEL > 0:

→ Inelastic events having at least one charged particle in $|\eta| < 1$

Midrapidity ($|\eta| < 0.5$) results

Forward rapidity ($-3.6 < \eta < -2.4$) results for the first time using tracks thanks to the newly installed MFT detector

$dN_{ch}/d\eta$ in pp collisions

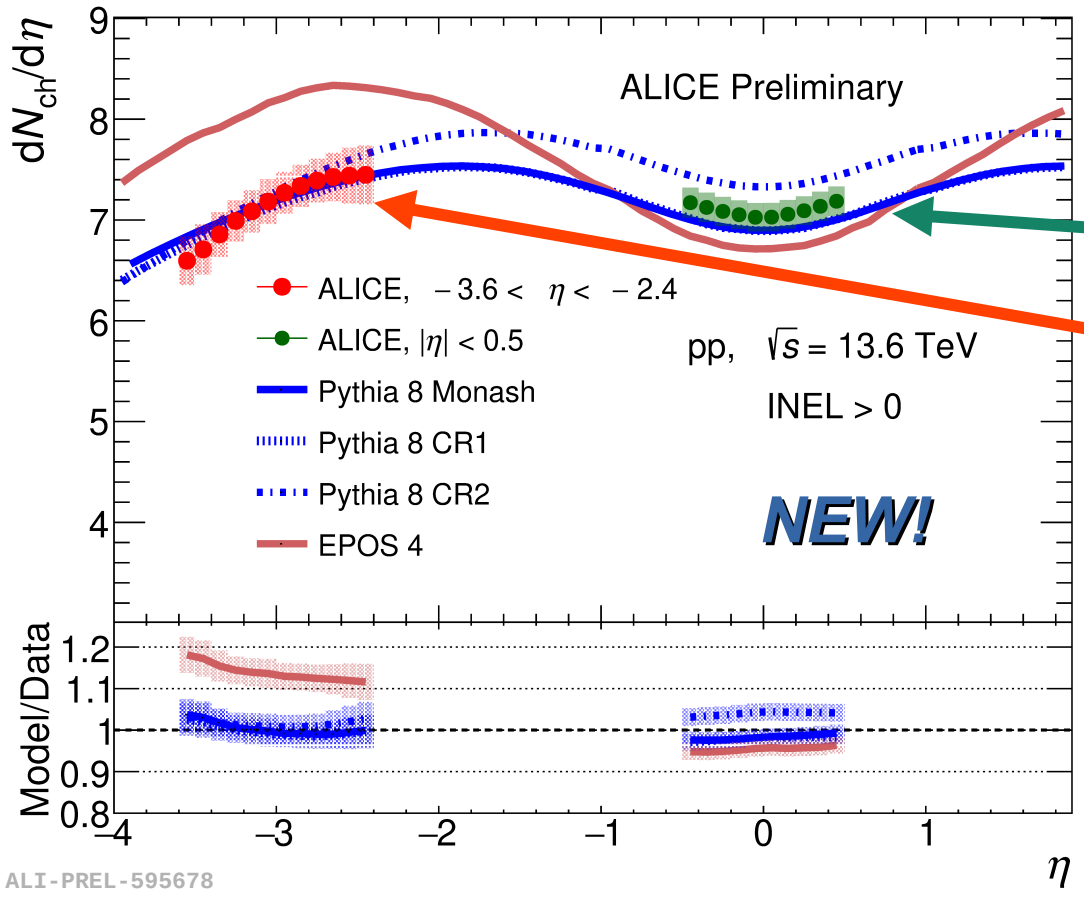

INEL > 0:

→ Inelastic events having at least one charged particle in $|\eta| < 1$

Midrapidity ($|\eta| < 0.5$) results

Forward rapidity ($-3.6 < \eta < -2.4$) results for the first time using tracks thanks to the newly installed MFT detector

PYTHIA 8

- → QCD strings with Lund fragmentation
- → Hadronisation mechanism: Color reconnection modes (Monash, CR1, CR2)

C. Bierlich et al. SPC 2022 (2022), 8

EPOS 4

- → Core–corona model + statistical hadronization
- → Collective effects: hydro-dynamical evolution

K. Werner, PRC 108 (2023) 064903

$dN_{ch}/d\eta$ in pp collisions

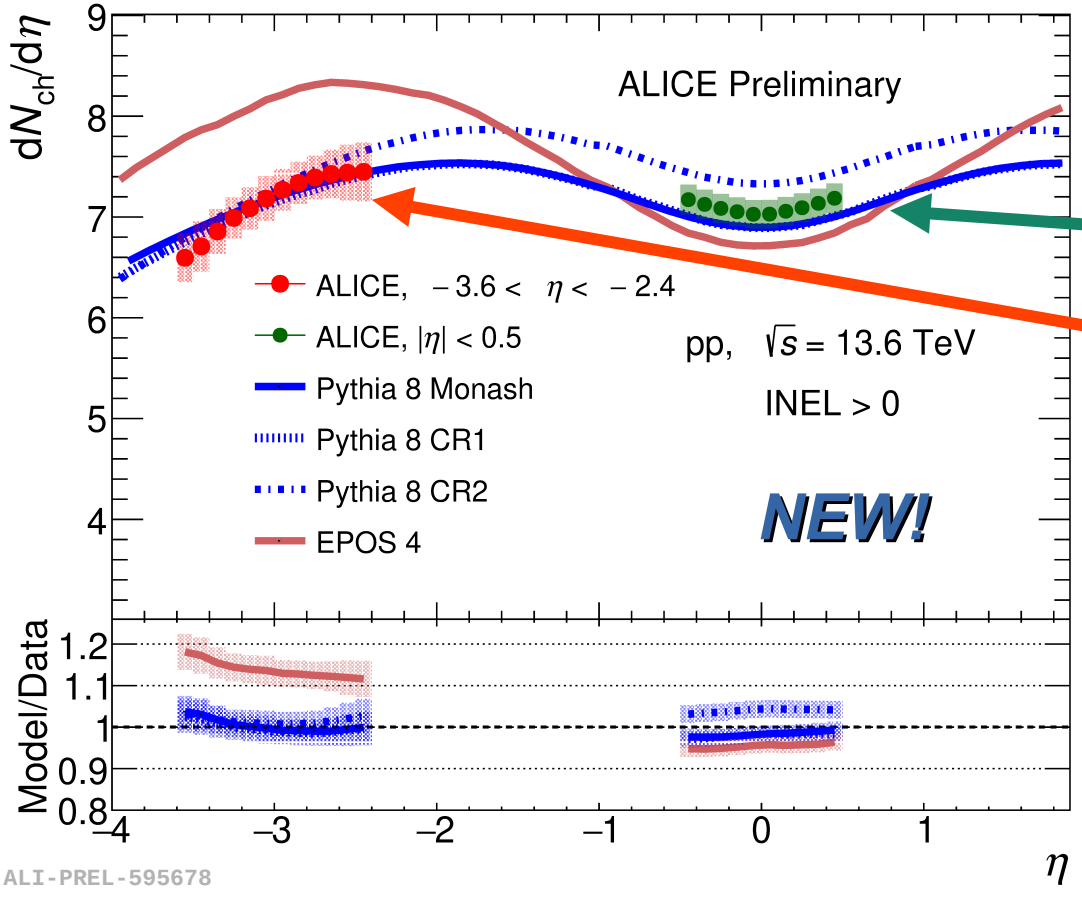

INEL > 0:

→ Inelastic events having at least one charged particle in $|\eta| < 1$

Midrapidity ($|\eta| < 0.5$) results

Forward rapidity ($-3.6 < \eta < -2.4$) results for the first time using tracks thanks to the newly installed MFT detector

PYTHIA 8

- → QCD strings with Lund fragmentation
- → Hadronisation mechanism: Color reconnection modes (Monash, CR1, CR2)

C. Bierlich et al. SPC 2022 (2022), 8

EPOS 4

- → Core–corona model + statistical hadronization
- → Collective effects: hydro-dynamical evolution

K. Werner, PRC 108 (2023) 064903

MC	$\|\eta\| < 0.5$	$-3.6 < \eta < -2.4$
PYTHIA	✓	✓
EPOS	✗	✗

$dN_{ch}/d\eta$ in pp collisions

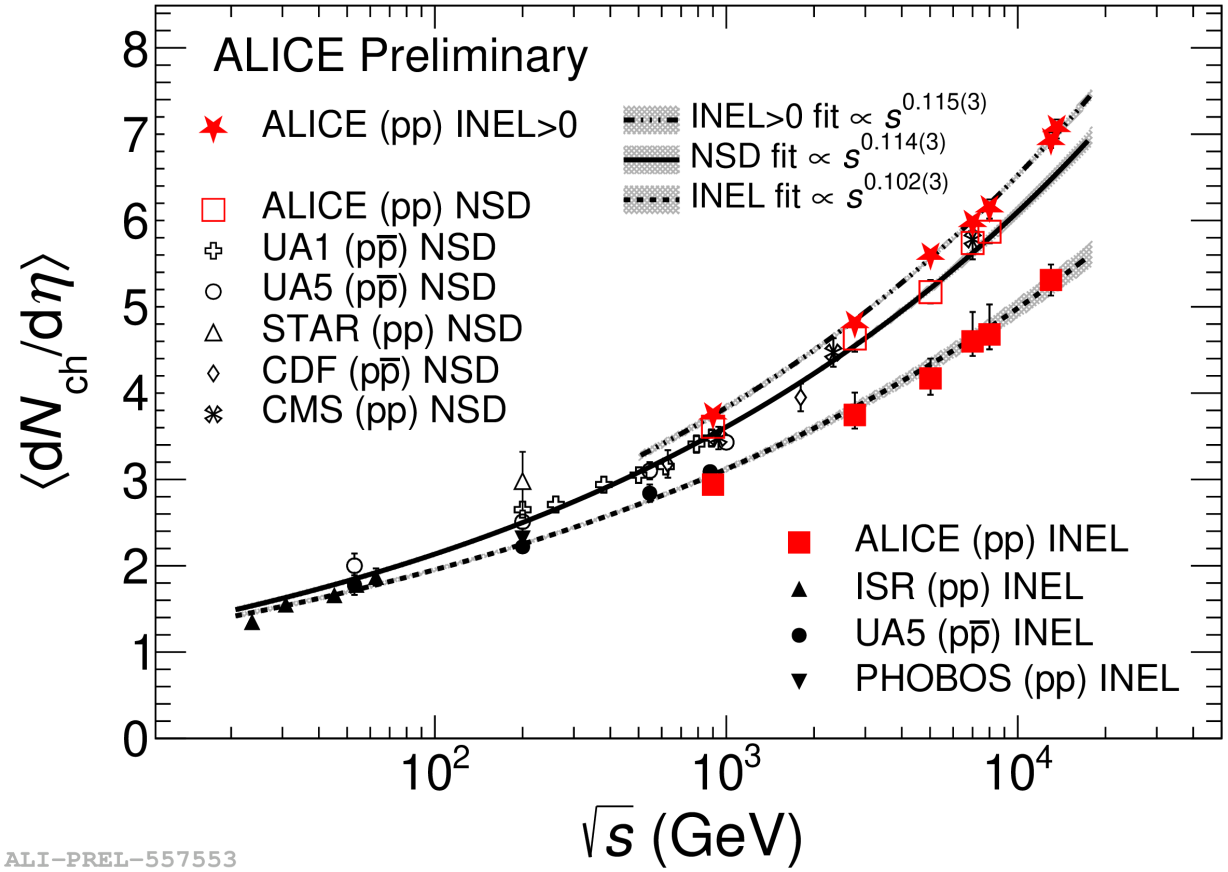

ALI-PREL-557553

$dN_{ch}/d\eta$ in pp collisions

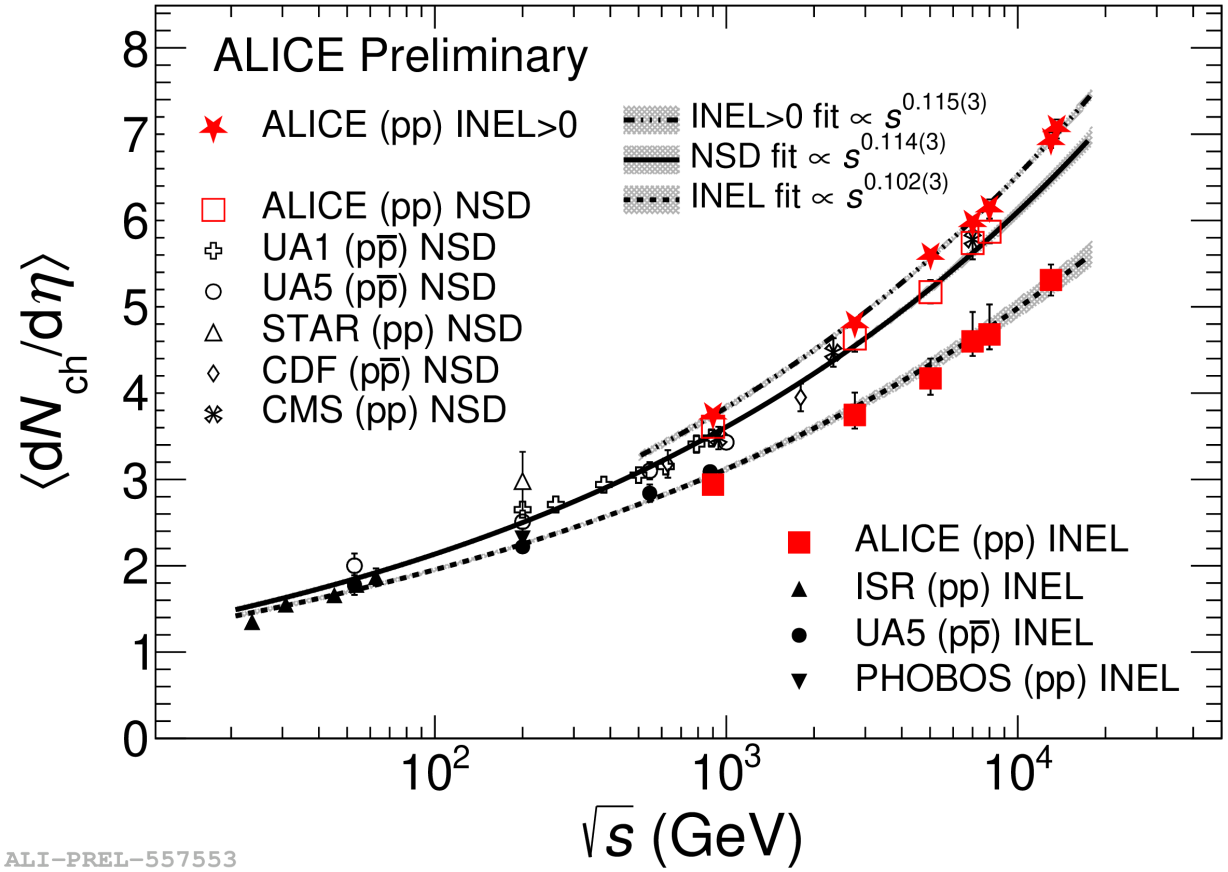

$\langle dN_{ch}/d\eta \rangle$:

→ $dN_{ch}/d\eta$ averaged over $|\eta| < 0.5$

$dN_{ch}/d\eta$ in pp collisions

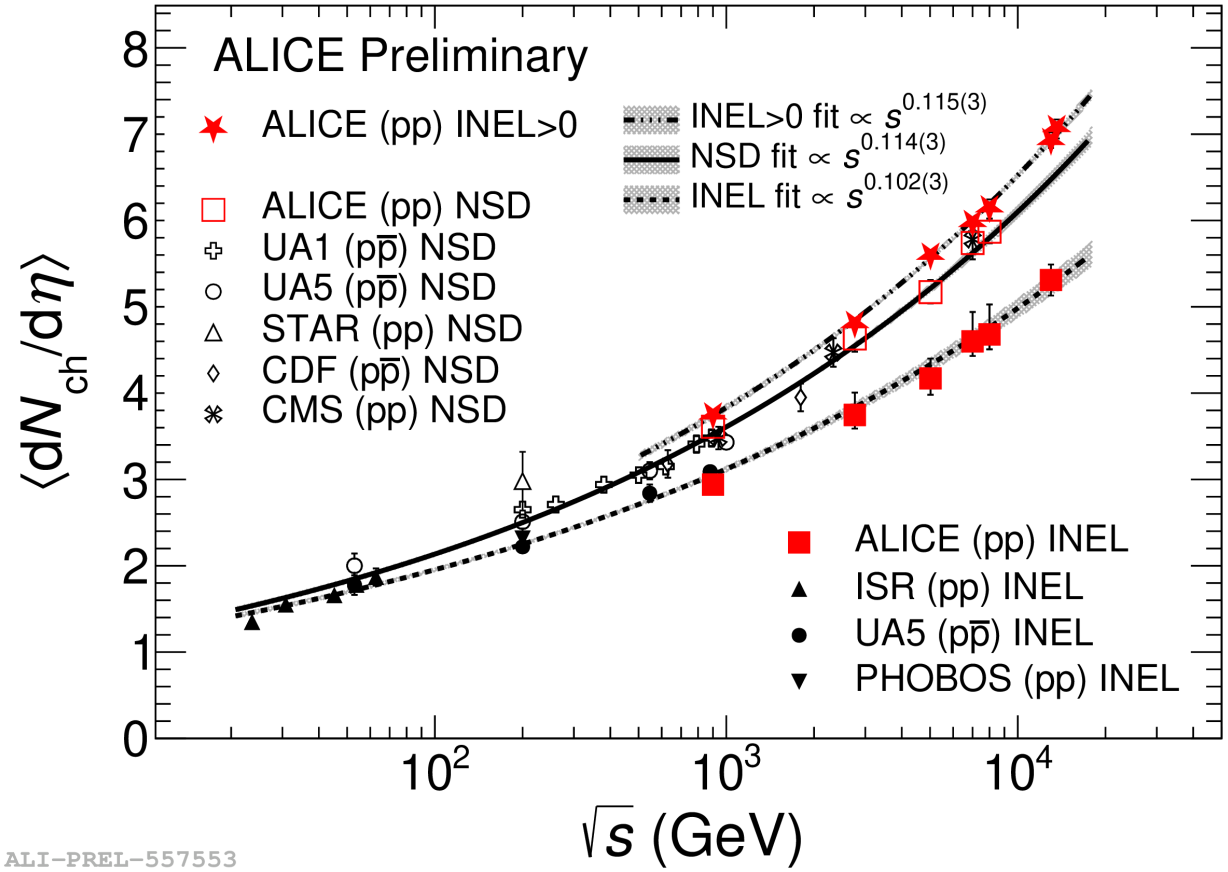

$\langle dN_{ch}/d\eta \rangle$:

→ $dN_{ch}/d\eta$ averaged over $|\eta| < 0.5$

$\langle dN_{ch}/d\eta \rangle$ vs $\sqrt{s}$

→ Power law dependence

→ INEL: $\propto s^{0.102}$

→ NSD: $\propto s^{0.114}$ [NSD: non-single diffractive]

→ INEL > 0: $\propto s^{0.115}$

$dN_{ch}/d\eta$ in pp collisions

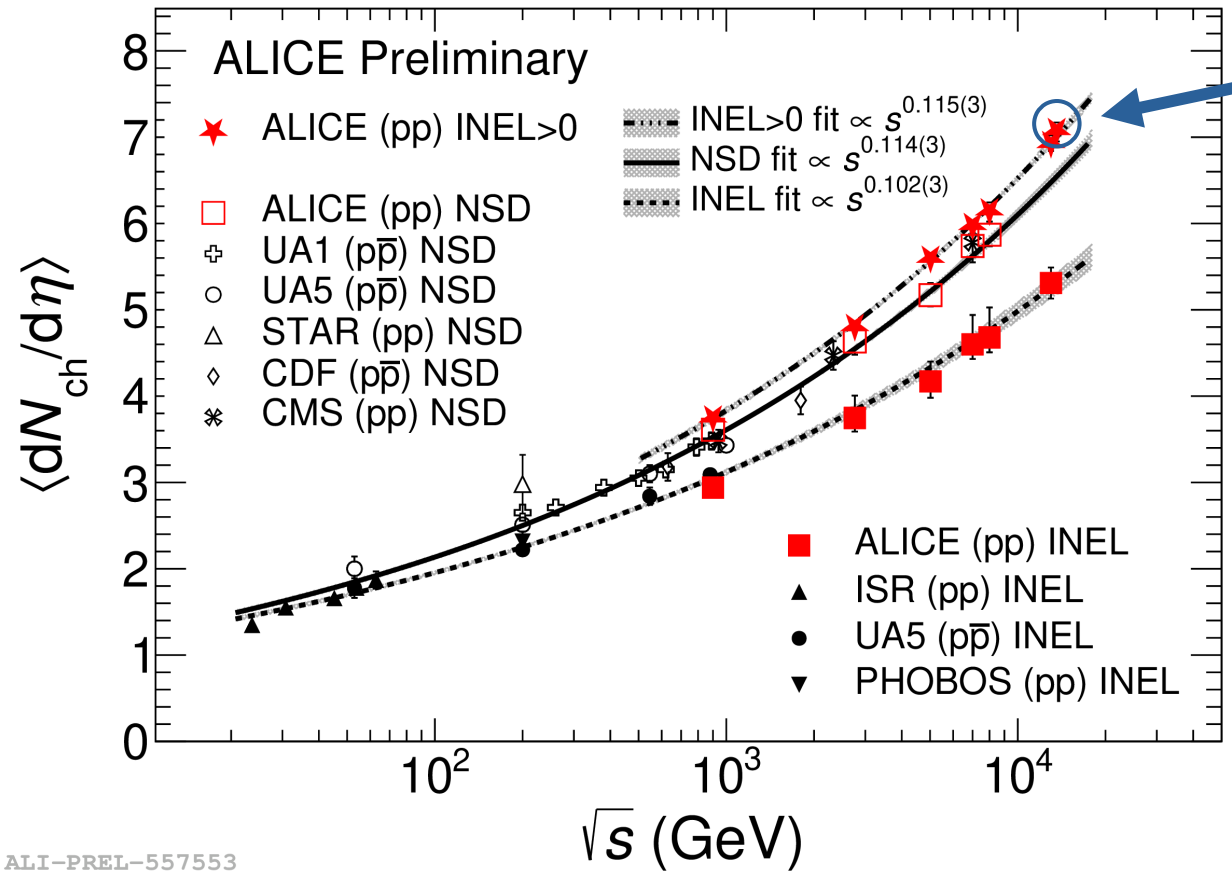

13.6 TeV

$\langle dN_{ch}/d\eta \rangle$:

→ $dN_{ch}/d\eta$ averaged over $|\eta| < 0.5$

$\langle dN_{ch}/d\eta \rangle$ vs $\sqrt{s}$

→ Power law dependence

→ INEL: $\propto s^{0.102}$

→ NSD: $\propto s^{0.114}$ [NSD: non-single diffractive]

→ INEL > 0: $\propto s^{0.115}$

$dN_{ch}/d\eta$ in pp collisions

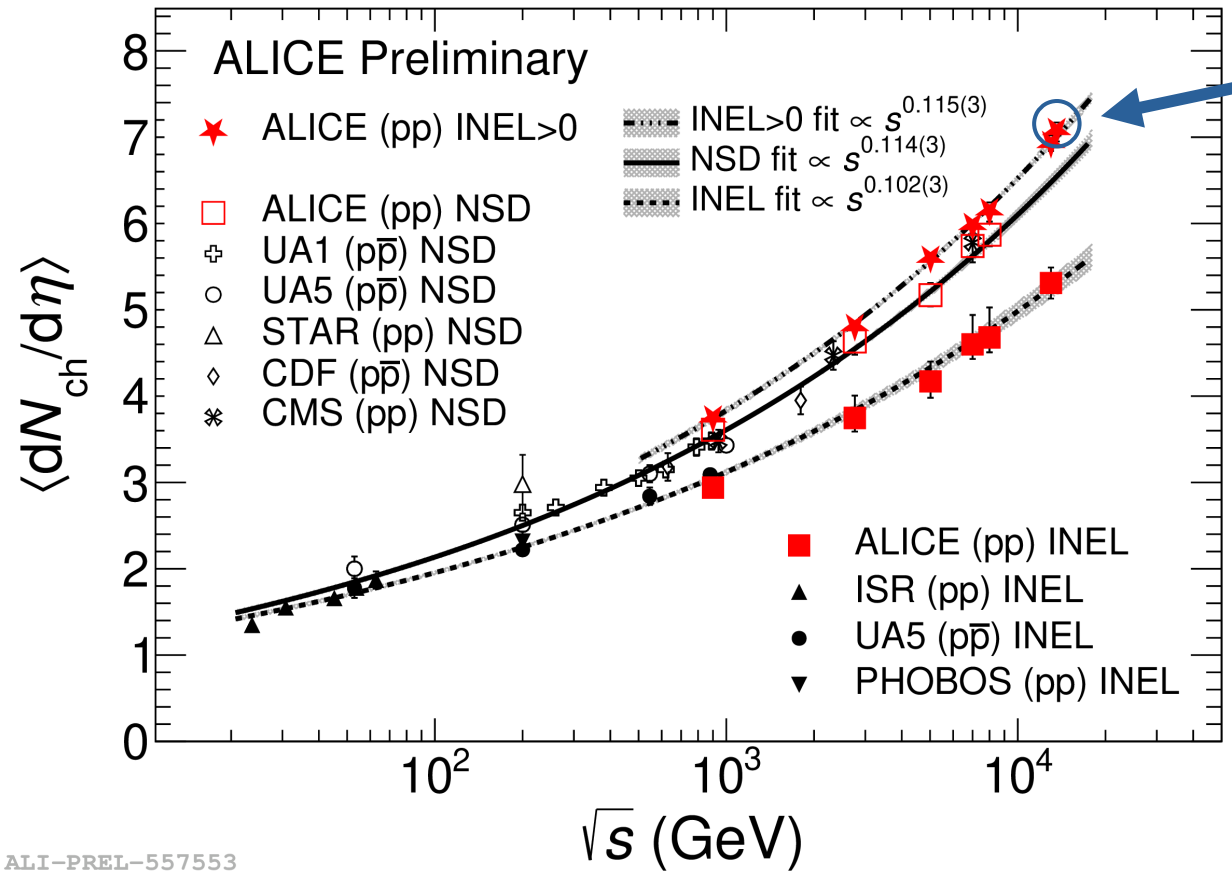

13.6 TeV

$\langle dN_{ch}/d\eta \rangle$:

→ $dN_{ch}/d\eta$ averaged over $|\eta| < 0.5$

$\langle dN_{ch}/d\eta \rangle$ vs $\sqrt{s}$

→ Power law dependence

→ INEL: $\propto s^{0.102}$

→ NSD: $\propto s^{0.114}$ [NSD: non-single diffractive]

→ INEL > 0: $\propto s^{0.115}$

New result is in agreement with expectations from previous measurements in pp collisions

Results from Pb–Pb collisions

$dN_{ch}/d\eta$ in Pb–Pb collisions

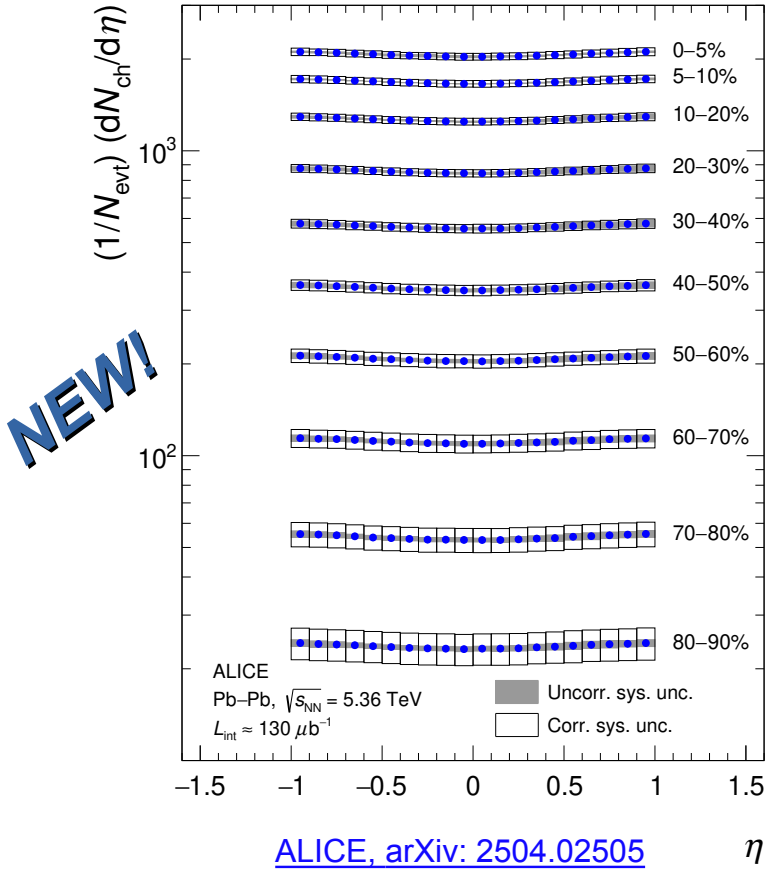

ALICE, arXiv: 2504.02505

Central

Peripheral

$dN_{ch}/d\eta$ for different centrality classes

ALI-PUB-602533

$dN_{ch}/d\eta$ in Pb–Pb collisions

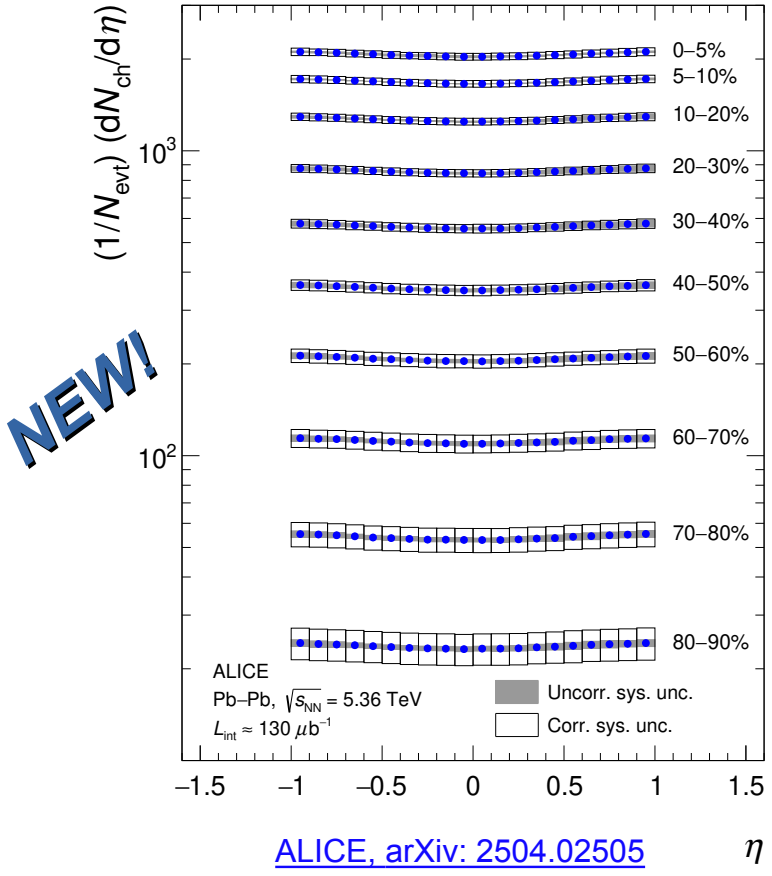

ALICE, arXiv: 2504.02505

ALI-PUB-602533

Central

Peripheral

$dN_{ch}/d\eta$ for different centrality classes

→ Rapid increase of $dN_{ch}/d\eta$ with collision centrality

$dN_{ch}/d\eta$ in Pb–Pb collisions

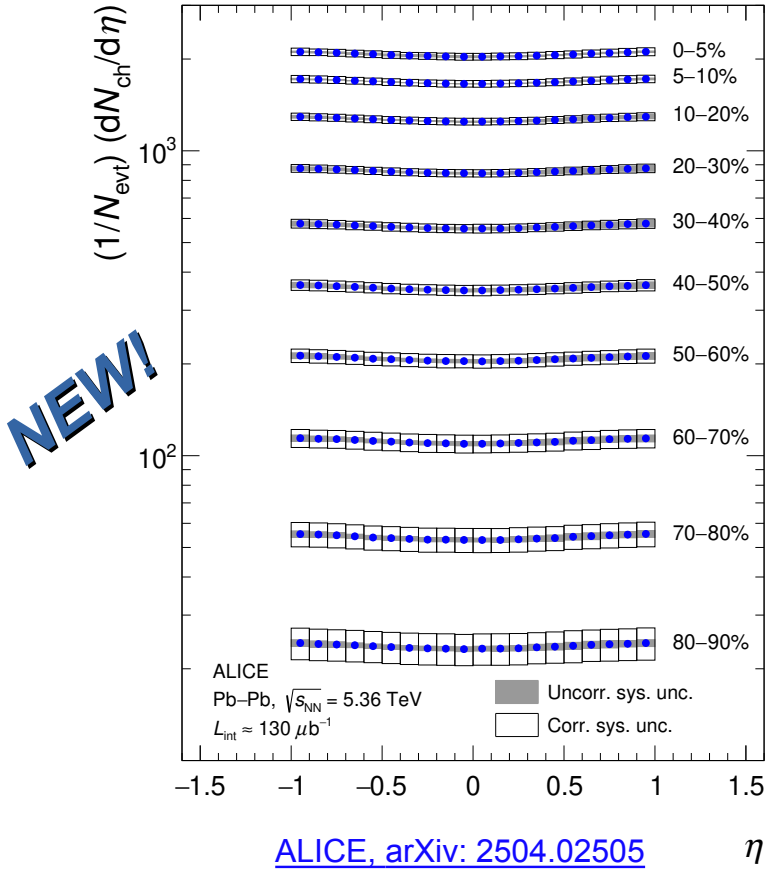

Central

Peripheral

$dN_{ch}/d\eta$ for different centrality classes

→ Rapid increase of $dN_{ch}/d\eta$ with collision centrality

→ $\langle dN_{ch}/d\eta \rangle$ = 2047 ± 54 (syst) for 0–5%

$dN_{ch}/d\eta$ in Pb–Pb collisions

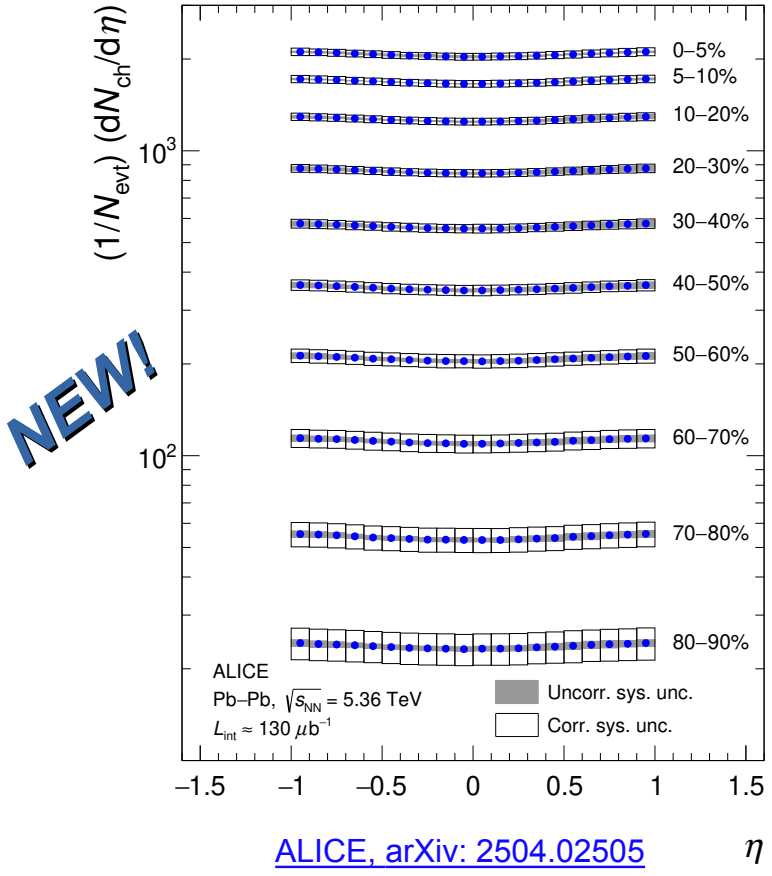

ALICE, arXiv: 2504.02505

ALI-PUB-602533

Central

Peripheral

$dN_{ch}/d\eta$ for different centrality classes

- → Rapid increase of $dN_{ch}/d\eta$ with collision centrality
- → $\langle dN_{ch}/d\eta \rangle$ = 2047 ± 54 (syst) for 0–5%
- → $\langle dN_{ch}/d\eta \rangle$ = 23.2 ± 2.8 (syst) for 80–90%

$dN_{ch}/d\eta$ in Pb–Pb collisions

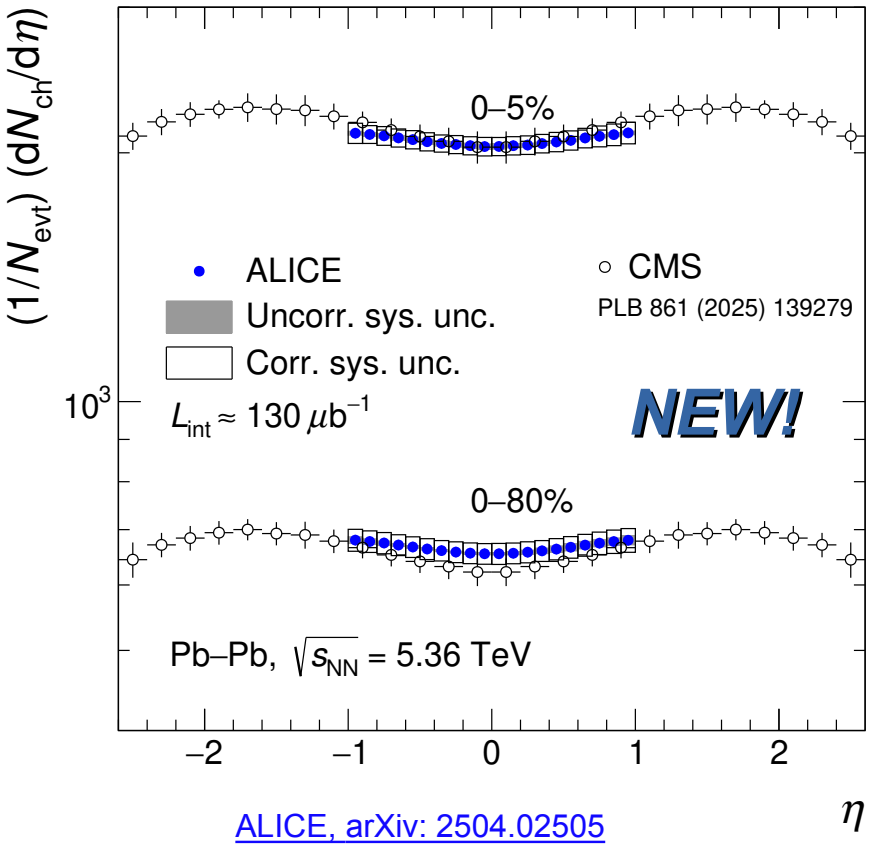

ALICE, arXiv: 2504.02505

ALI-PUB-602538

ALICE

→ Multiplicity-based centrality estimator

CMS

→ Transverse energy based centrality estimator

Results from two experiments are consistent with each other

$dN_{ch}/d\eta$ in Pb–Pb collisions

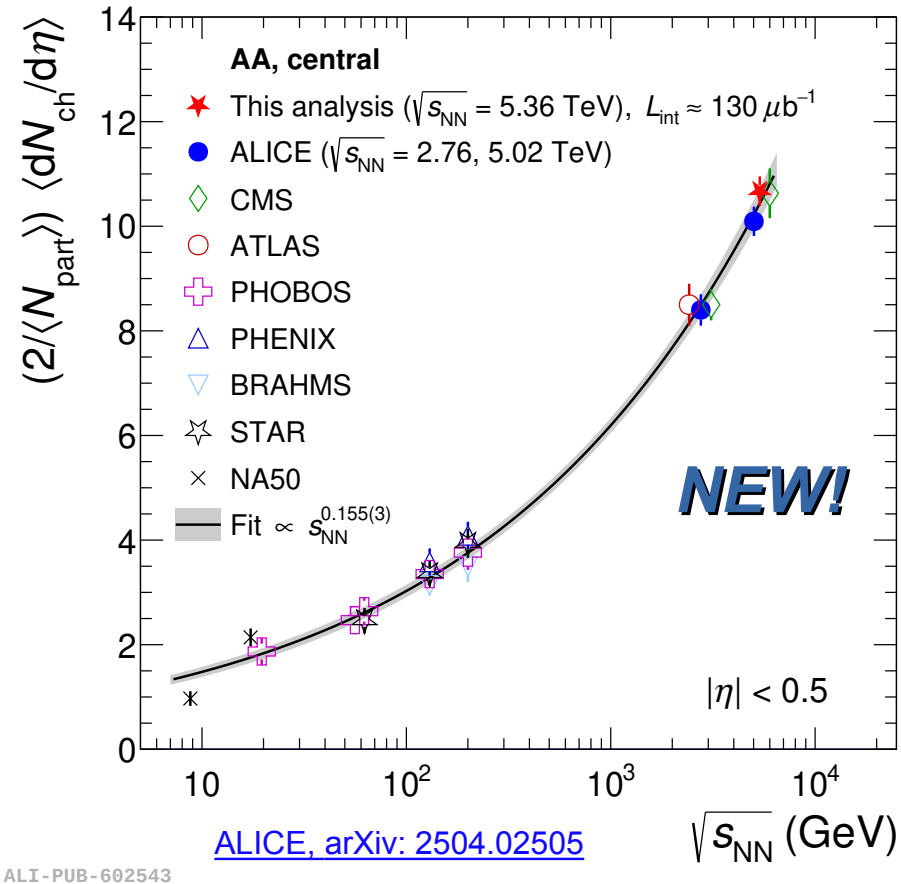

$(2/\langle N_{part}\rangle)\langle dN_{ch}/d\eta\rangle$ vs $\sqrt{s_{NN}}$

→ Power law dependence

→ $\propto s_{NN}^{0.155}$

→ Heavy-ion collisions exhibit a steeper energy dependence than in pp ($\propto s^{0.115}$)

$dN_{ch}/d\eta$ in Pb–Pb collisions

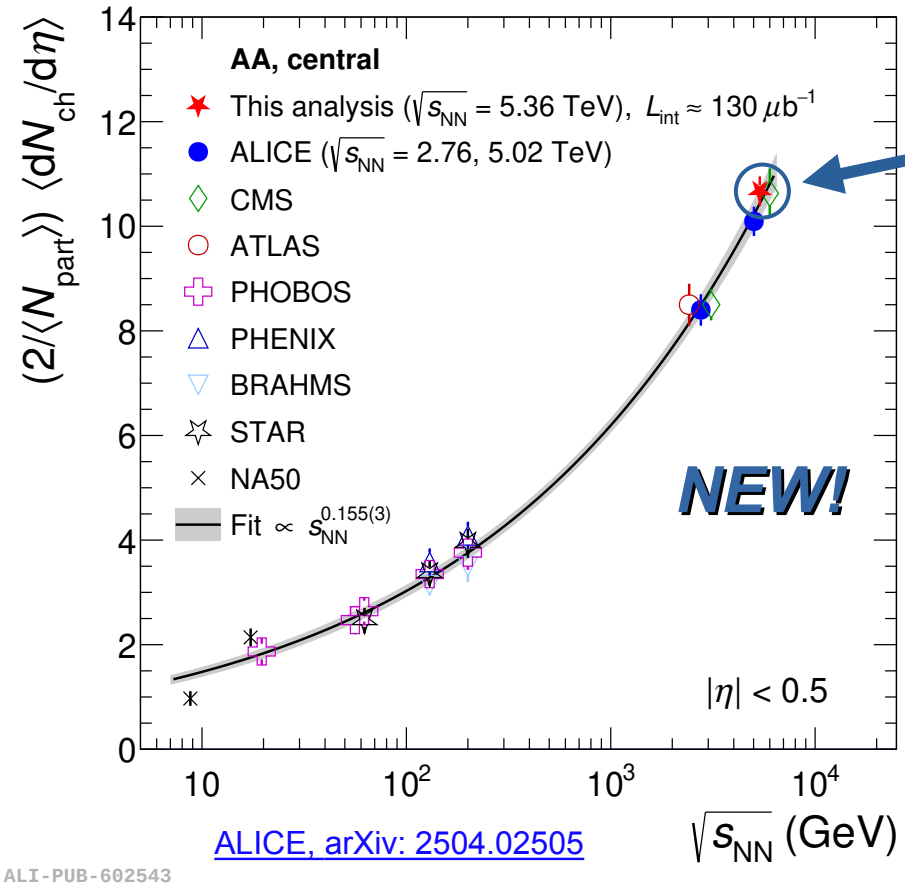

5.36 TeV

$(2/\langle N_{part}\rangle)\langle dN_{ch}/d\eta\rangle$ vs $\sqrt{s_{NN}}$

→ Power law dependence

→ $\propto s_{NN}^{0.155}$

→ Heavy-ion collisions exhibit a steeper energy dependence than in pp ($\propto s^{0.115}$)

$dN_{ch}/d\eta$ in Pb–Pb collisions

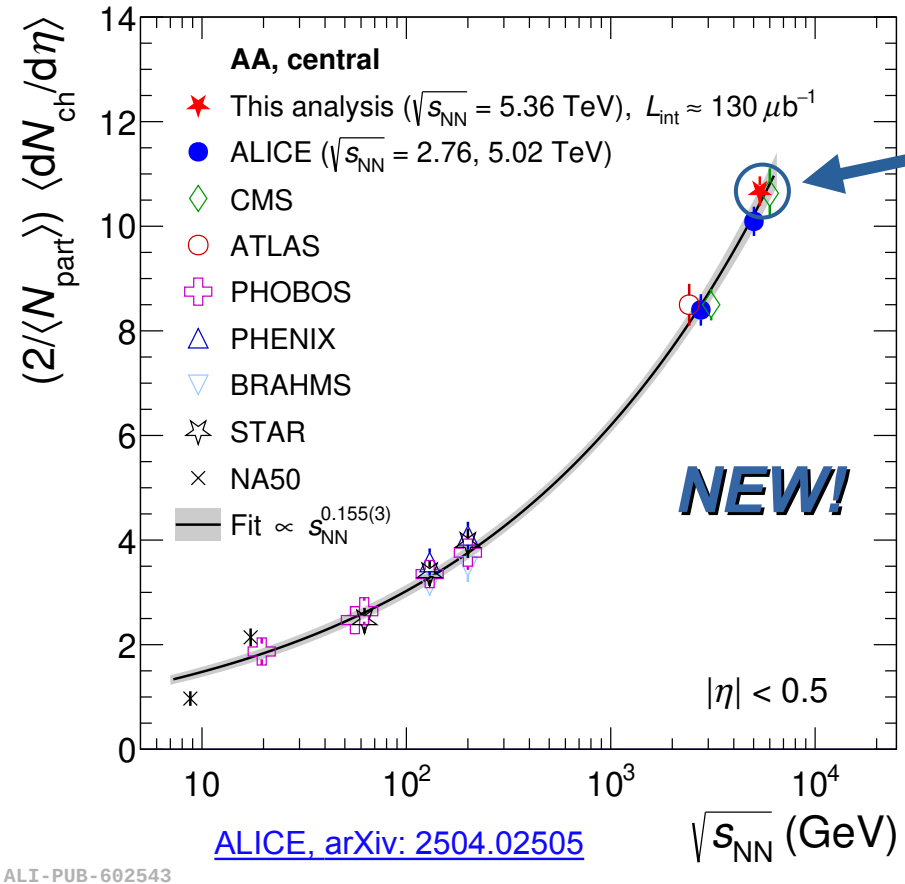

ALI-PUB-602543

5.36 TeV

$(2/\langle N_{part}\rangle)\langle dN_{ch}/d\eta\rangle$ vs $\sqrt{s_{NN}}$

→ Power law dependence

→ $\propto s_{NN}^{0.155}$

→ Heavy-ion collisions exhibit a steeper energy dependence than in pp ($\propto s^{0.115}$)

Results agree with lower energy measurements in heavy-ion collisions

$dN_{ch}/d\eta$ in Pb–Pb collisions

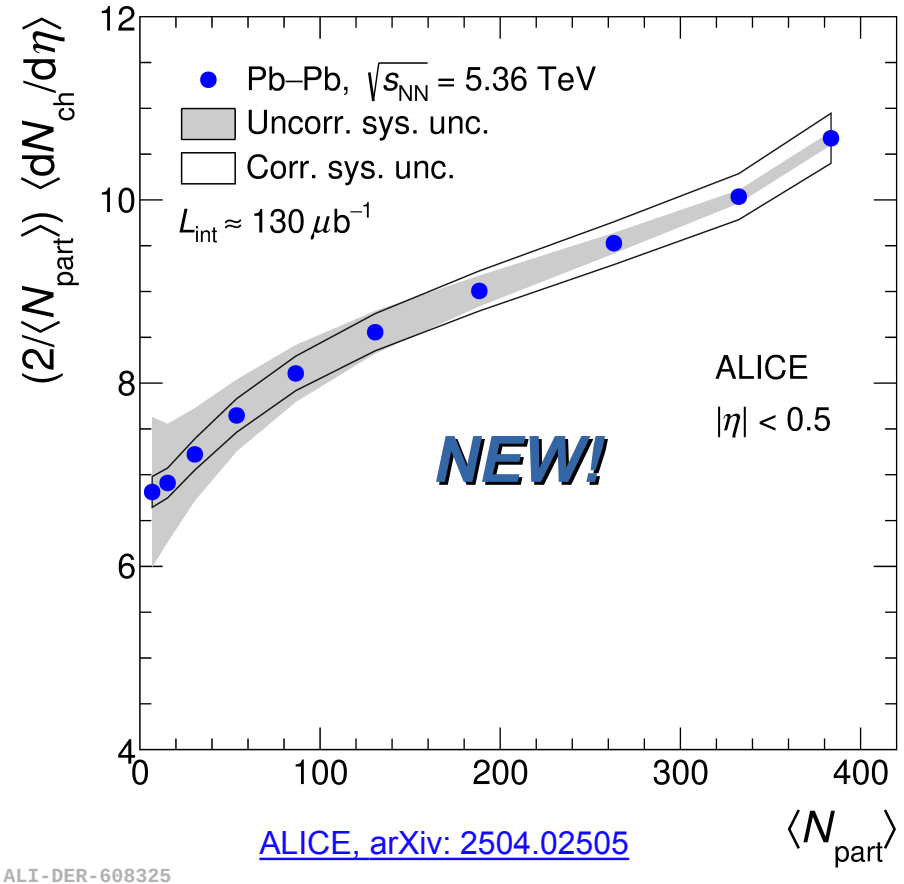

ALICE, arXiv: 2504.02505

ALI-DER-608325

$(2/\langle N_{part}\rangle)\langle dN_{ch}/d\eta\rangle$ vs centrality

→ Factor ~1.8 increase in multiplicity from peripheral to central events

$dN_{ch}/d\eta$ in Pb–Pb collisions

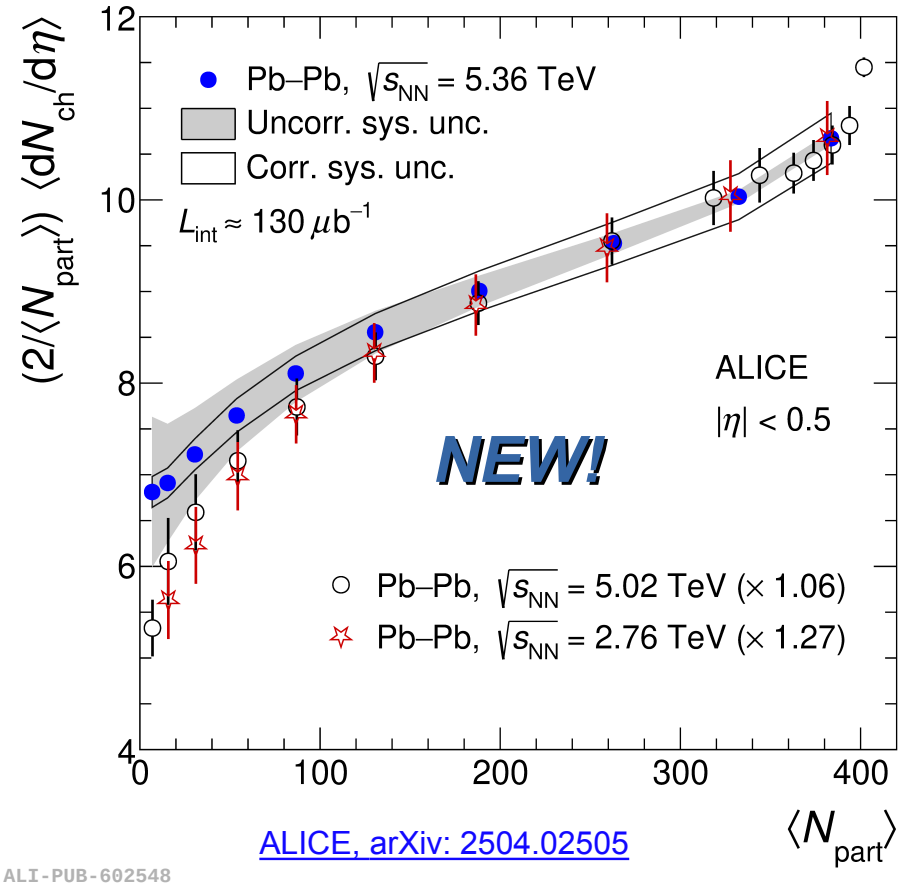

ALICE, arXiv: 2504.02505

ALI-PUB-602548

$(2/\langle N_{part}\rangle)\langle dN_{ch}/d\eta\rangle$ vs centrality

- → Factor ~1.8 increase in multiplicity from peripheral to central events
- → Similar centrality dependence at all LHC energies

$dN_{ch}/d\eta$ in Pb–Pb collisions

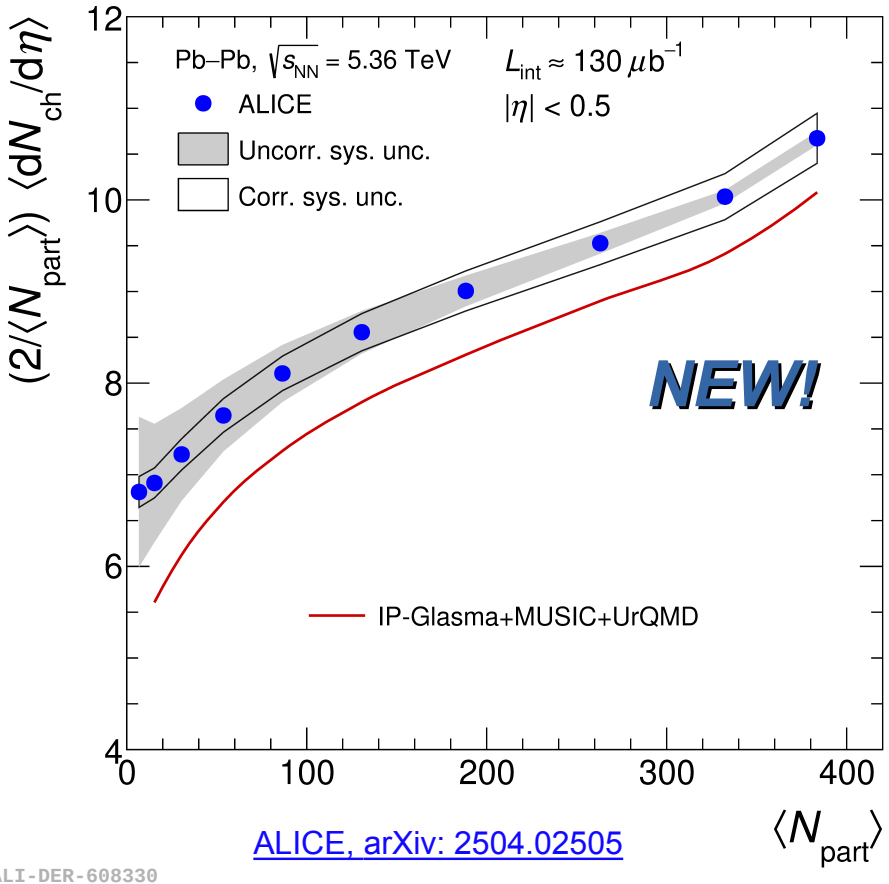

ALICE, arXiv: 2504.02505

ALI-DER-608330

IP-Glasma: Based on Color Glass Condensate (CGC) to describe the initial distribution of gluons inside the nuclei

Hydrodynamic model: **MUSIC** *B. Schenke et al. PRL 108 (2012) 252301*

Hadronic cascade: **UrQMD** *B. Schenke et al. PRC 102 (2020) 034905*

$dN_{ch}/d\eta$ in Pb–Pb collisions

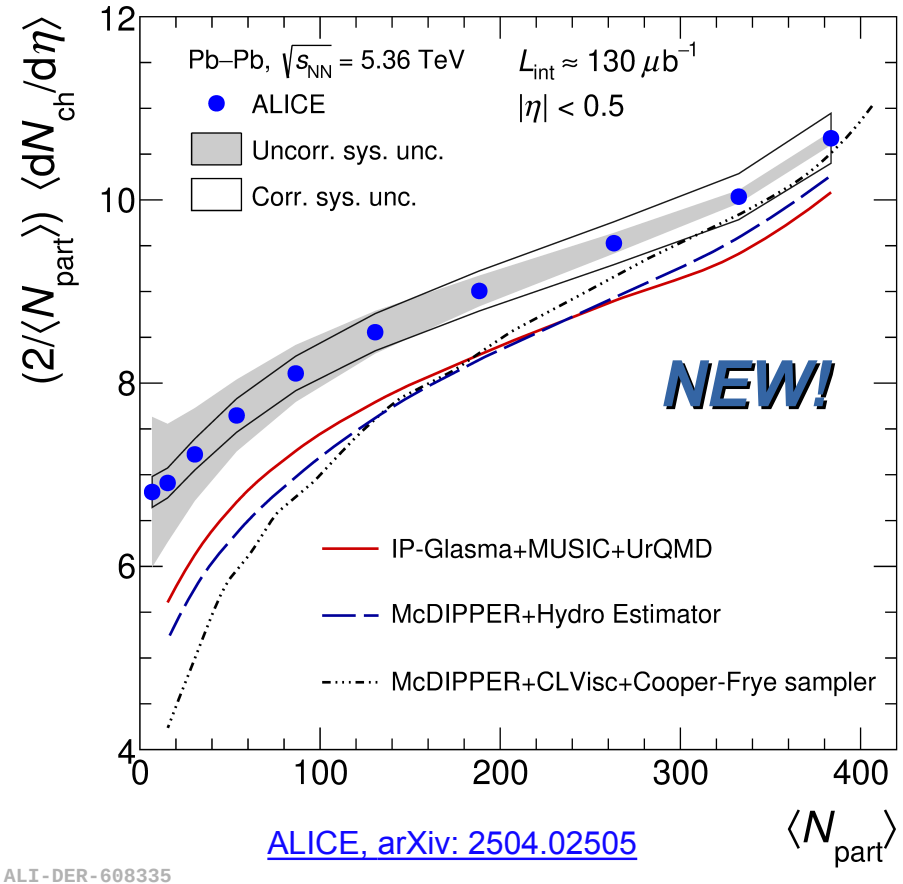

ALICE, arXiv: 2504.02505

ALI-DER-608335

IP-Glasma: Based on Color Glass Condensate (CGC) to describe the initial distribution of gluons inside the nuclei
Hydrodynamic model: **MUSIC**
Hadronic cascade: **UrQMD**

B. Schenke et al. PRL 108 (2012) 252301
B. Schenke et al. PRC 102 (2020) 034905

McDIPPER: Based on leading-order cross section calculations within the CGC
Hydrodynamic model: **CLVisc**
Hadronic cascade: **Cooper-Frye sampler**

O. Garcia-Montero et al. PRC 109 (2024) 044916
G. Giacalone et al. PRL 123 (2019) 262301
O. Garcia-Montero et al. arXiv:2501.14872

$dN_{ch}/d\eta$ in Pb–Pb collisions

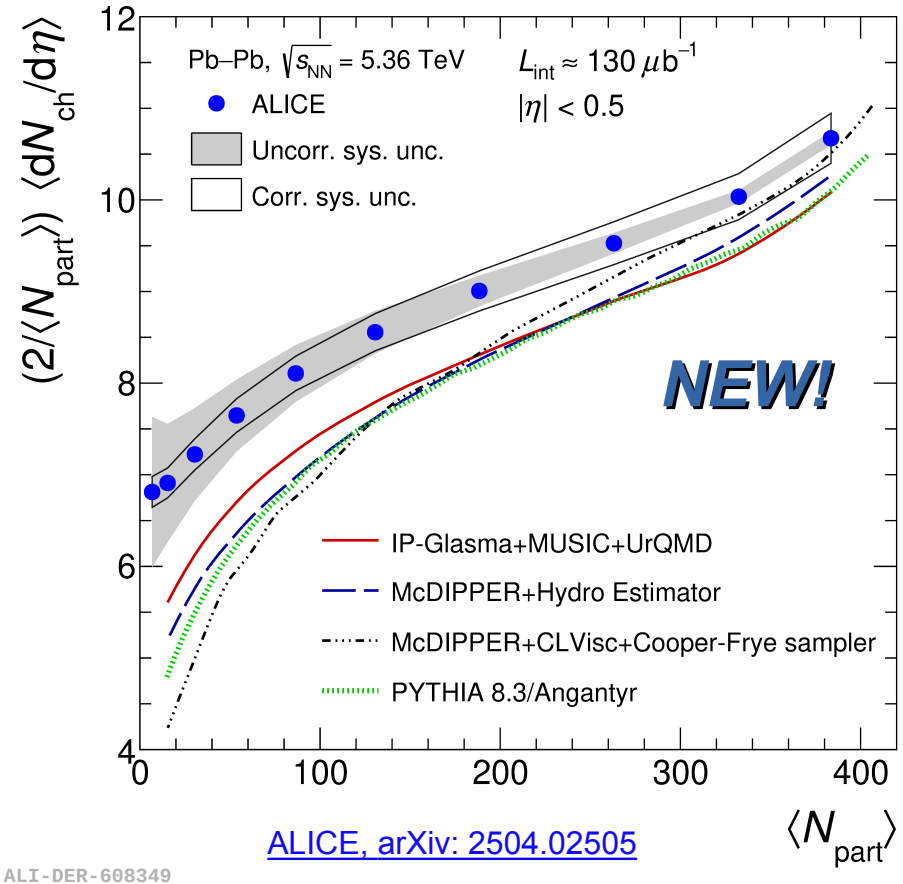

ALICE, arXiv: 2504.02505

ALI-DER-608349

IP-Glasma: Based on Color Glass Condensate (CGC) to describe the initial distribution of gluons inside the nuclei
Hydrodynamic model: **MUSIC**
Hadronic cascade: **UrQMD**

B. Schenke et al. PRL 108 (2012) 252301
B. Schenke et al. PRC 102 (2020) 034905

McDIPPER: Based on leading-order cross section calculations within the CGC
Hydrodynamic model: **CLVisc**
Hadronic cascade: **Cooper-Frye sampler**

O. Garcia-Montero et al. PRC 109 (2024) 044916
G. Giacalone et al. PRL 123 (2019) 262301
O. Garcia-Montero et al. arXiv:2501.14872

PYTHIA Angantyr: Modelling individual nucleon-nucleon interactions, no quark-gluon plasma (QGP)

C. Bierlich et al.JHEP 10 (2018) 134

$dN_{ch}/d\eta$ in Pb–Pb collisions

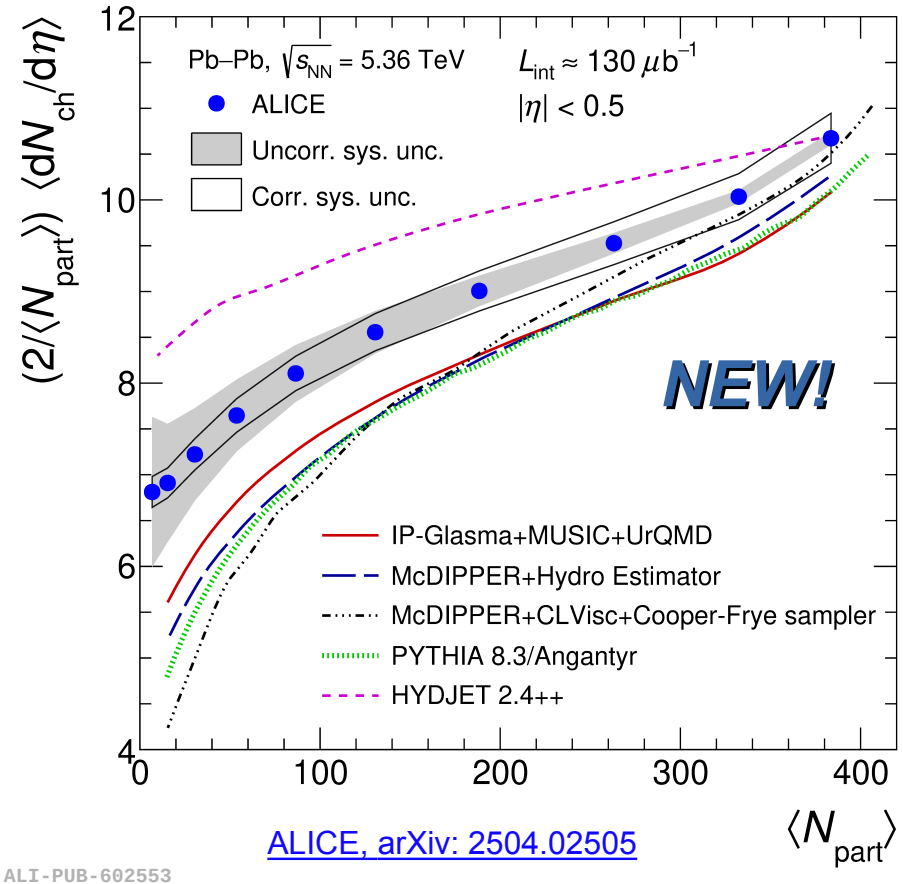

ALICE, arXiv: 2504.02505

ALI-PUB-602553

IP-Glasma: Based on Color Glass Condensate (CGC) to describe the initial distribution of gluons inside the nuclei
Hydrodynamic model: **MUSIC**
Hadronic cascade: **UrQMD**

B. Schenke et al. PRL 108 (2012) 252301
B. Schenke et al. PRC 102 (2020) 034905

McDIPPER: Based on leading-order cross section calculations within the CGC
Hydrodynamic model: **CLVisc**
Hadronic cascade: **Cooper-Frye sampler**

O. Garcia-Montero et al. PRC 109 (2024) 044916
G. Giacalone et al. PRL 123 (2019) 262301
O. Garcia-Montero et al. arXiv:2501.14872

PYTHIA Angantyr: Modelling individual nucleon-nucleon interactions, no quark-gluon plasma (QGP)

C. Bierlich et al.JHEP 10 (2018) 134

HYDJET: Full evolution of heavy-ion collisions (jet interaction, QGP, hadronic phase)

I. P. Lokhtin et al. Comput. Phys. Commun. 180 (2009) 779–799

$dN_{ch}/d\eta$ in Pb–Pb collisions

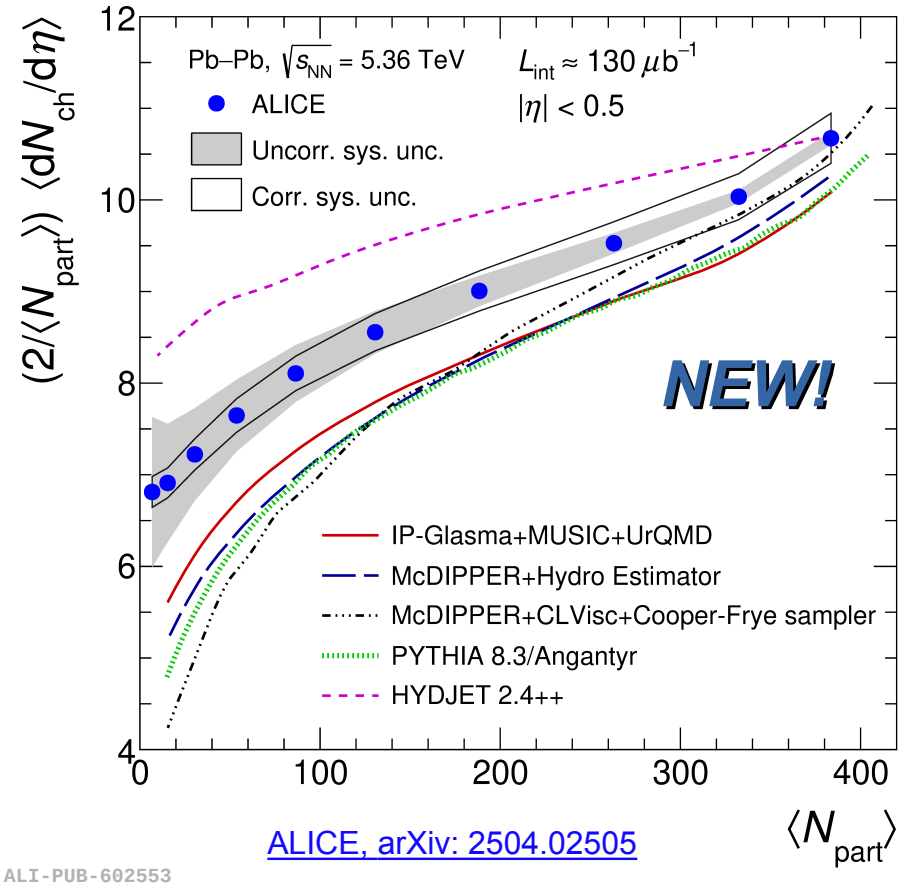

ALICE, arXiv: 2504.02505

ALI-PUB-602553

IP-Glasma: Based on Color Glass Condensate (CGC) to describe the initial distribution of gluons inside the nuclei
Hydrodynamic model: **MUSIC**
Hadronic cascade: **UrQMD**

B. Schenke et al. PRL 108 (2012) 252301
B. Schenke et al. PRC 102 (2020) 034905

McDIPPER: Based on leading-order cross section calculations within the CGC
Hydrodynamic model: **CLVisc**
Hadronic cascade: **Cooper-Frye sampler**

O. Garcia-Montero et al. PRC 109 (2024) 044916
G. Giacalone et al. PRL 123 (2019) 262301
O. Garcia-Montero et al. arXiv:2501.14872

PYTHIA Angantyr: Modelling individual nucleon-nucleon interactions, no quark-gluon plasma (QGP)

C. Bierlich et al.JHEP 10 (2018) 134

HYDJET: Full evolution of heavy-ion collisions (jet interaction, QGP, hadronic phase)

I. P. Lokhtin et al. Comput. Phys. Commun. 180 (2009) 779–799

Good performance of these models in central collisions but discrepancy in peripheral collisions

Summary and outlook

- Charged-particle multiplicity was measured using upgraded ITS, TPC and newly installed MFT detector, showing good performance of upgraded ALICE experimental setup
- Results from new LHC energy show good compatibility with earlier measurements
- New input for constraining theoretical models

Looking forward to new exciting results with
O–O, p–O and Ne–Ne data

Thanks for your kind attention!